



Technische Universität München

School of Computation, Information and Technology



Master's Thesis

Resolvent-based Methods for Robust Spectral Analysis in Dynamical Systems

April Herwig

april.herwig@tum.de

Supervisor: Prof Oliver Junge

Submission Date:

I assure the single handed composition of this master's thesis only supported by declared resources.

Garching,

Abstract

Koopmania

Contents

1	Introduction	1
2	Background	1
2.1	Koopman and Perron-Frobenius Operators	1
2.2	Spectral Properties	4
2.2.1	The Spectrum	4
2.2.2	Spectra of Koopman and Perron-Frobenius Operators .	6
2.3	Pseudospectra	8
2.3.1	Definitions of the Pseudospectrum	9
2.3.2	Properties	12
3	Numerical Methods	15
3.1	Petrov-Galerkin Methods	15
3.2	Extended Dynamic Mode Decomposition (EDMD)	16
3.2.1	The Galerkin Ansatz	16
3.2.2	Functional Minimization	17
3.2.3	EDMD for the Perron-Frobenius Operator	18
3.3	Residual EDMD (ResDMD)	19
3.3.1	Validation of Koopman Eigenpairs	19
3.3.2	A Naive Attempt at Duality	22
3.4	kernel EDMD (kEDMD)	24
3.4.1	The Kernel Trick	24
3.4.2	Application to EDMD	26
3.5	kernel ResDMD (kResDMD)	28
3.5.1	Associating a Residual to \hat{K}	28
3.5.2	The Perron-Frobenius Connection	30
4	Benchmark Examples	30
4.1	Duffing Oscillator	31
4.2	Alanine Dipeptide	31
4.3	Blaschke Products	33
4.3.1	Definition	33
4.3.2	An Initial Numerical Experiment	35
4.3.3	The Adjoint of $H^2(A)$	36
5	Conclusion	39
References		40

1 Introduction

Dynamical systems theory has seen many revolutions. One recent such revolution is to use operator theoretic tools to analyze the global behavior of chaotic systems. Conceived in the 1930's by Koopman and Von Neumann [18], the study of global dynamics under a mapping S is conducted by studying the action of the composition $\psi \circ S$ of S with an observable ψ . Observables which act as eigenvalues for the composition operator and its dual hold information on slowly decaying structures in phase space.

Currently the most popular method by far for analyzing composition operators (named Koopman operators) is dynamic mode decomposition (DMD). The past 2 decades have seen massive growth in this topic, and DMD has received many evolutions [8]. One primary concern of nearly all DMD methods is *spectral pollution*. The Koopman operator often has unfavorable spectral qualities such as continuous spectrum which are unstable, and are destroyed by finite approximation. The task presented in the present paper is to identify which candidate eigenvalues (computed e.g. by DMD) are approximations of eigenvalues of the true Koopman operator (or its adjoint), and which arise due to discretization.

2 Background

We consider a discrete dynamical system generated by a map $S : \Omega \rightarrow \Omega$ defined on a measure space $(\Omega, \mathcal{A}, dx)$ which is *nonsingular*, that is $\int_{S^{-1}(A)} dx = 0$ for any $A \in \mathcal{A}$ with $\int_A dx = 0$.

2.1 Koopman and Perron-Frobenius Operators

Koopman operator theory shifts the focus from dynamics of points in state space \mathcal{X} to dynamics of observables $g : \Omega \rightarrow \mathbb{C}$. A state $x \in \Omega$ evolves by iteratively applying the map S , and similarly observables evolve under the action of the *Koopman operator*

$$\mathcal{K}g = g \circ S. \quad (2.1)$$

The primary benefit of this alternative viewpoint of dynamics is that \mathcal{K} is *linear* and can therefore be analyzed using algebraic and functional analytic tools. However, the Koopman operator acts on function spaces which are typically infinite-dimensional. Even the Krylov space $\{g, \mathcal{K}g, \mathcal{K}^2g, \dots\}$ is generically infinite-dimensional: consider e.g. an indicator function $g = \mathbb{1}_{[0,1]}$ and a translation $S(x) = x - 1$.

It should be noted that until now we have not declared a function space to act as a domain for \mathcal{K} . This is because there are many potential domains for which \mathcal{K} is not only well-defined, but has interesting properties worth studying. For the current section we consider $\mathcal{K} : L^\infty \rightarrow L^\infty$. On this space \mathcal{K} is obviously bounded, in fact it is a contraction. However, that need not be the case for other spaces. Depending one the function space and in S , \mathcal{K} may not even be bounded.

The Koopman operator tracks how observables evolve with S . There is however a dual viewpoint: that of *densities* and *pushforwards*. From the duality pairing

$$\langle f, \mathcal{K}g \rangle = \langle \mathcal{L}f, g \rangle \quad (2.2)$$

for $f \in L^1$, $g \in L^\infty$ we may deduce the form of an adjoint operator, known as the *transfer operator* or *Perron-Frobenius operator*. Consider an indicator $g = \mathbb{1}_A$ for an $A \in \mathcal{A}$ and let $f \geq 0$. The left hand side of 2.2 is

$$\int f(x) \mathbb{1}_A(S(x)) dx = \int f(x) \mathbb{1}_{S^{-1}(A)}(x) dx = \int_{S^{-1}(A)} f(x) dx, \quad (2.3)$$

and the right hand side

$$\int \mathcal{L}f(x) \mathbb{1}_A(x) dx = \int_A \mathcal{L}f(x) dx. \quad (2.4)$$

Hence $\mathcal{L}f \in L^1$ should satisfy the equation

$$\int_A \mathcal{L}f(x) dx = \int_{S^{-1}(A)} f(x) dx. \quad (2.5)$$

A short exercise in measure theory shows that

$$A \mapsto \int_{S^{-1}(A)} f(x) dx \quad (2.6)$$

defines a finite absolutely continuous measure, and hence by the Radon-Nikodym theorem the measure has a unique density which by 2.5 is precisely $\mathcal{L}f$. For general $f \in L^1$ decompose $f = f^+ - f^-$ with $f^+, f^- \geq 0$ and set $\mathcal{L}f = \mathcal{L}f^+ - \mathcal{L}f^-$.

2.6 shows that \mathcal{L} is precisely the action of the pushforward $S_\sharp\mu = \mu \circ S^{-1}$ for densities. This provides a useful intuition for the transfer operator: we move away from the viewpoint of single points $x \in \Omega$, and instead consider

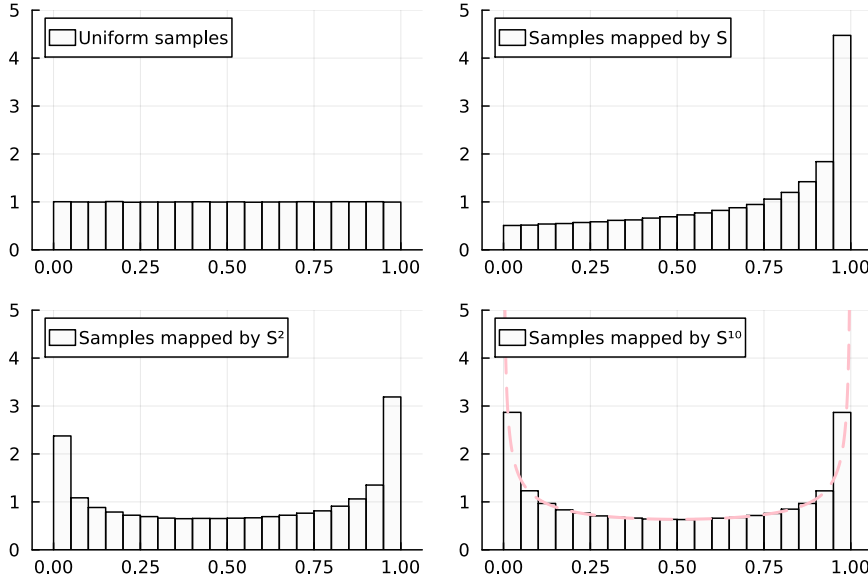


Figure 2.1: Illustration of the pushforward intuition of the Perron-Frobenius operator. Action of the \mathcal{L} associated with the quadratic map $S : [0, 1] \circlearrowleft$, $x \mapsto 4x(1 - x)$. One million points are sampled uniformly in $[0, 1]$ and mapped forward under S , S^2 , and S^{10} . The respective distributions are shown in histograms.

distributions of point density. If x is chosen from a random distribution with density f , then the distribution of $S(x)$ has density $\mathcal{L}f$.

When S is a diffeomorphism, \mathcal{L} has an explicit form.

Theorem 2.1. *Let S be a diffeomorphism. Then*

$$\mathcal{L}f = \frac{f \circ S^{-1}}{|\det D S^{-1}|} \quad (2.7)$$

In particular one sees that when S is a measure algebra isomorphism (that is, S and S^{-1} both preserve the measure) then the Koopman operator is unitary, i.e. $\mathcal{K}^*(=\mathcal{L}) = \mathcal{K}^{-1}$.

Proof. This follows from a change of variables $y = S(x)$

$$\int g \cdot \mathcal{L}f \, dx = \int \mathcal{K} \cdot f \, dx = \int f(y) \cdot g \circ S^{-1}(y) |\det D S(S^{-1}(y))| \, dy. \quad (2.8)$$

□

Corollary 2.2. *Assume S is a piecewise diffeomorphism, i.e. there exists a disjoint decomposition $\Omega = \biguplus_{l=1}^n U_l$ such that for each l , $S_l := S|_{U_l} : U_l \rightarrow V_l$*

is a diffeomorphism. Then

$$(\mathcal{L}f)(x) = \sum_{l=1}^n \frac{f \circ S_l^{-1}(x)}{|\det D S_l^{-1}(x)|} \mathbb{1}_{V_l}(x). \quad (2.9)$$

2.2 Spectral Properties

2.2.1 The Spectrum

We begin with abstract definitions for parts of the spectrum.

Definition 2.3. Let $M : D(M) \rightarrow \mathcal{X}$ be a linear operator on a Banach space $(X, \|\cdot\|)$. The domain $D(M) \subset \mathcal{X}$ of M may be a dense subset of \mathcal{X} . M is called closed if: whenever $x_k \rightarrow x$ is a convergent sequence with Mx_k convergent, then $Mx_k \rightarrow Mx$.

Closedness is weaker than continuity due to the extra assumption that Mx_k is convergent.

Definition 2.4. The spectrum $\sigma(M)$ of a closed operator M is the set of numbers $\lambda \in \mathbb{C}$ for which $M - \lambda I$ does not have a bounded inverse. The complement $\rho(M) := \mathbb{C} \setminus \sigma(M)$ is called resolvent set and $(M - \lambda I)^{-1}$ is called the resolvent.

Proposition 2.5. The spectrum admits a disjoint decomposition

$$\sigma(M) = \sigma_p(M) \uplus \sigma_c(M) \uplus \sigma_r(M) \quad (2.10)$$

into point-, continuous-, and residual-spectrum with

$$\sigma_p(M) = \{\lambda \in \mathbb{C} \mid M - \lambda I \text{ is not injective}\}, \quad (2.11)$$

$$\sigma_c(M) = \{\lambda \in \mathbb{C} \mid M - \lambda I \text{ is injective, but its range is a dense subset of } \mathcal{X}\}, \quad (2.12)$$

$$\sigma_r(M) = \{\lambda \in \mathbb{C} \mid M - \lambda I \text{ is injective, but does not have dense range}\}. \quad (2.13)$$

Remark. In some literature, 0 is never part of the spectrum. We do not take this approach.

An element $\lambda \in \sigma_p(M)$ is a *true* eigenvalue in the sense that there exists a vector $x \in \mathcal{X}$ such that $(M - \lambda I)x = 0$. The continuous spectrum has a similar characterization as the set of $\lambda \in \mathbb{C}$ for which $M_\lambda I$ is injective but *not* bounded from below, i.e. there exists a sequence $(x_k)_k$, $\|x_k\| = 1$, for which $(M - \lambda I)x_k \rightarrow 0$. Equivalently, $(M - \lambda I)^{-1}$ cannot be extended to a bounded linear operator, but is still a (densely defined) closed linear operator. (See the proof of theorem 2.20 for a proof of this characterization.)

We have already used the duality pairing 2.2 to deduce a form of the Perron-Frobenius operator. For completeness we provide a full definition for the adjoint of an unbounded operator and cite some basic facts about adjoints.

Definition 2.6. Let $M : \mathcal{X} \supset D(M) \rightarrow \mathcal{X}$ be a densely defined closed linear operator on a Banach space. The adjoint operator is constructed as follows. Let

$$D(M^*) = \{f \in \mathcal{X}^* \mid \exists f' \in \mathcal{X} : \langle f, Mg \rangle = \langle f', g \rangle \quad \forall g \in D(M)\}. \quad (2.14)$$

Now M^* is defined by $M^*f = f'$.

Lemma 2.7 ([17]). Let \mathcal{X} be a reflexive¹ Banach space. Then the adjoint operator is also densely defined and closed, and

1. $M^{**} = M$,
2. $\ker(M^*) = \text{ran}(M)^\perp$,

where for $A \subset \mathcal{X}$, $A^\perp = \{f \in \mathcal{X}^* \mid \langle f, g \rangle = 0 \quad \forall g \in A\}$ is the annihilator.

One might ask why such detail is required in defining the spectrum. The answer lies in the subtle consequences of infinite-dimensionality. The following example from [14] shows the subtle interplay between residual spectrum and spectrum of the adjoint operator, all of which requires infinite-dimensionality.

Example 2.8 (Shift operators on $\ell^2(\mathbb{N})$). The canonical right-shift operator

$$R : (a_1, a_2, \dots) \mapsto (0, a_1, a_2, \dots) \quad (2.15)$$

is adjoint to the left shift

$$L : (a_1, a_2, \dots) \mapsto (a_2, a_3, \dots). \quad (2.16)$$

We claim:

$$\sigma_p(L) = \{\lambda \in \mathbb{C} \mid |\lambda| < 1\} \quad \sigma_p(R) = \emptyset \quad (2.17)$$

$$\sigma_c(L) = \{\lambda \in \mathbb{C} \mid |\lambda| = 1\} \quad \sigma_c(R) = \{\lambda \in \mathbb{C} \mid |\lambda| = 1\} \quad (2.18)$$

$$\sigma_r(L) = \emptyset \quad \sigma_r(R) = \{\lambda \in \mathbb{C} \mid |\lambda| < 1\}. \quad (2.19)$$

Indeed, to see 2.17 consider $|\lambda| < 1$, $a^\lambda = (\lambda, \lambda^2, \dots)$. Then clearly $La^\lambda = \lambda a^\lambda$. On the other hand, suppose $Ra = \lambda a$ for some $a \neq 0$, $\lambda \in \mathbb{C}$. Then letting n be the first index such that $a_n \neq 0$, we must have $0 = a_{n-1} = (Ra)_n = \lambda a_n$ so $\lambda = 0$. But the kernel of R is clearly $\{0\}$.

¹The bidual \mathcal{X}^{**} is isomorphic to \mathcal{X} , that is, $\mathcal{X}^{**} \cong \mathcal{X}$.

To see 2.18, take $|\lambda| = 1$ and construct *approximate* (L, λ) -eigenvectors $v^n = (\lambda, \lambda^2, \dots, \lambda^n, 0, \dots)$. Then $(L - \lambda I)v^n = (0, \dots, 0, \lambda^{n+1}, 0, \dots)$ so $\|(L - \lambda I)v^n\| = 1$ but $\|v^n\| = \sqrt{n}$. It remains to show that λ is of continuous spectrum, as opposed to residual spectrum. Indeed, for any w such that for all $v \in \ell^2$, $0 = \langle (L - \lambda I)v, w \rangle = \langle v, (R - \bar{\lambda}I)w \rangle$ so that w is an eigenvector of R which by 2.17 is a contradiction. An entirely analogous argument shows that the circle is also continuous spectrum for R .

We now reverse the discussion to see that any $|\lambda| < 1$ is in the residual spectrum of R . For $v \in \ell^2$ and w a $\bar{\lambda}$ -eigenvector of L we have $0 = \langle v, 0 \rangle = \langle v, (L - \bar{\lambda}I)w \rangle = \langle (R - \lambda I)v, w \rangle$ so that the range of $R - \lambda I$ is orthogonal to w .

Finally, $\sigma(M)$ is bounded by $\|M\|$ for any operator M , and clearly $\|L\| = 1$. But $\sigma_p(L) \cup \sigma_c(L) = \{\lambda \in \mathbb{C} \mid |\lambda| \leq 1\}$ so $\sigma_r(L) = \emptyset$. Combined with the previous paragraph, this shows 2.19.

The example already suggests some important relationships regarding the spectrum of adjoint operators.

Theorem 2.9. *Let M be a densely defined closed linear operator on a reflexive Banach space.*

1. $\lambda \in \sigma(M)$ iff $\bar{\lambda} \in \sigma(M^*)$.
2. If $\lambda \in \sigma_r(M)$, then $\bar{\lambda} \in \sigma_p(M^*)$.
3. Conversely, if $\lambda \in \sigma_p(M)$, then $\bar{\lambda} \in \sigma_p(M^*) \cup \sigma_r(M^*)$.
4. $\sigma_c(M) = \sigma_c(M^*)$.

Proof. 1. Suppose $M - \lambda I$ has a bounded inverse B . Then $(M - \lambda I)B = B(M - \lambda I) = I$. Equivalently $B^*(M^* - \bar{\lambda}I) = (M^* - \bar{\lambda}I)B^* = I^* = I$.

2. The range of $M - \lambda I$ is not dense in \mathcal{X} . Hence there exists a $v \in \text{ran}(M - \lambda I)^\perp$. But this implies $v \in \ker(M^* - \bar{\lambda}I)$.
3. There exists a $v \in \ker(M - \lambda I)$ which implies $v \in \text{ran}(M^* - \bar{\lambda}I)^\perp$.
4. Follows from 1, 2, and 3.

□

2.2.2 Spectra of Koopman and Perron-Frobenius Operators

The Koopman and Perron-Frobenius operator spectrum holds information about the long-term mixing rates of structures in phase space. We write (with some abuse of notation) $\mathcal{L}|_{\mathcal{X}}$ and $\mathcal{K}|_{\mathcal{X}}$ to denote the Perron-Frobenius / Koopman operators acting on the domain \mathcal{X} .

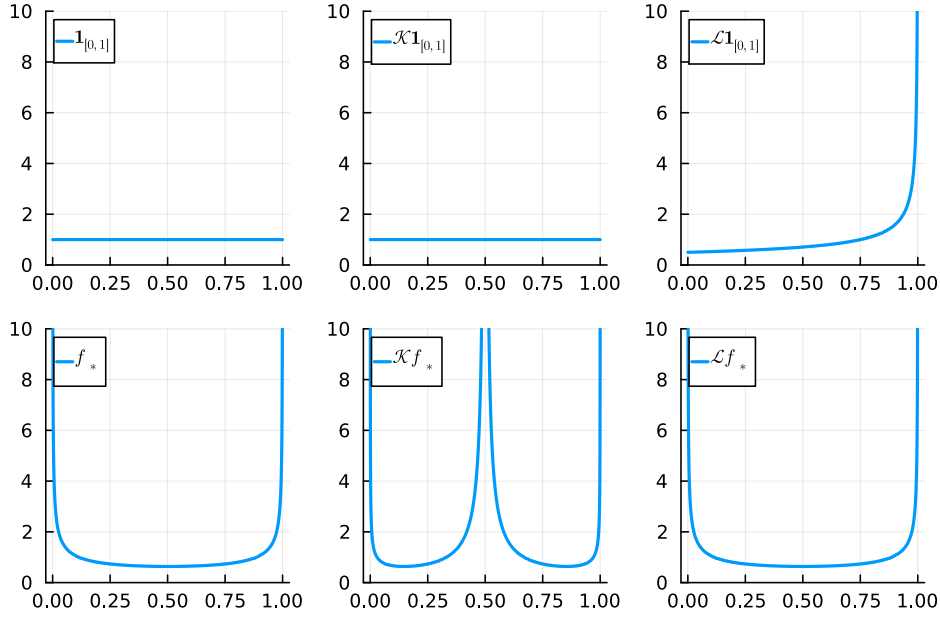


Figure 2.2: Actions of the Koopman and Perron-Frobenius operators associated with the quadratic map $S : [0, 1] \circlearrowleft, x \mapsto 4x(1-x)$. The constant density $\mathbb{1}_{[0,1]}$ is fixed under \mathcal{K} and the density $f_*(x) = \frac{1}{\pi\sqrt{x(1-x)}}$ is fixed under \mathcal{L} (c.f. figure 2.1).

Definition 2.10. An eigenfunction f for $\mathcal{L}|_{L^1}$ with eigenvalue 1 is the density of a (signed) invariant measure. We say S preserves the measure $f dx$.

The following are well-known facts about the Koopman and Perron-Frobenius operator. They can be found in many sources e.g. [20].

Theorem 2.11. 1. If S is ergodic², then there is at most one invariant density. Conversely, if there is a unique invariant density which is $(dx-)$ almost everywhere positive, then S is ergodic.

- 2. If S is ergodic, then every eigenvalue of $\mathcal{K}|_{L^1}$ is simple.
- 3. Suppose S is invertible. Then S is weak-mixing iff 1 is the only eigenvalue of $\mathcal{K}|_{L^1}$.

The following theorem is from [12].

Definition 2.12. A set $A \subset \Omega$ in phase space is called δ -almost-invariant if

$$\int_{S^{-1}(A) \cap A} dx = (1 - \delta) \cdot \int_A dx. \quad (2.20)$$

²Ergodicity and mixing describe how observations become decorrelated over time. S is ergodic if for all $A, B \in \mathcal{A}$ we have $\frac{1}{n} \sum_{j=0}^{n-1} \int_{S^{-j}(A) \cap B} dx \rightarrow \int_A dx \int_B dx$ as $n \rightarrow \infty$. S is weak-mixing if we have $\frac{1}{n} \sum_{j=0}^{n-1} \left| \int_{S^{-j}(A) \cap B} dx - \int_A dx \int_B dx \right| \rightarrow 0$ as $n \rightarrow \infty$.

Theorem 2.13. Let $\mathbb{R} \ni \lambda < 1$ be an eigenvalue corresponding to a real-valued normalized eigenfunction f of $\mathcal{L}|_{L^1}$. Let further $A \subset \Omega$ be such that $\int_A f dx = \frac{1}{2}$. Then

$$\delta + \eta = \lambda + 1 \quad (2.21)$$

if A is δ -almost-invariant and $\Omega \setminus A$ is η -almost-invariant.

These are only a few interesting properties of the spectrum of these operators, but there are many more which can be studied.

2.3 Pseudospectra

The reader will have likely noticed the sensitivity required in understanding the spectrum for infinite-dimensional operators. In particular the spectral types can be unstable w.r.t. perturbations of the operator. For example, for any self-adjoint operator M (e.g. the generator for the Koopman semigroup in a continuous-time dynamical system) there exists a compact operator E with arbitrarily small norm such that the perturbation $M + E$ has purely point spectrum.

The situation is even worse when one considers *perturbations of the dynamics* instead of perturbations of the Koopman / Perron-Frobenius operators. Consider a circle rotation $S : \mathbb{T} \rightarrow \mathbb{T}$, $e^{2\pi i \theta} \mapsto e^{2\pi i(\theta+\alpha)}$. We have $\sigma(\mathcal{L}|_{L^2}) = \sigma_p(\mathcal{L}|_{L^2}) = \alpha^{\mathbb{N}_0}$. If the rotation is rational then the spectrum is discrete, but if the rotation is irrational then the spectrum is dense in the unit circle.

In the present paper we tackle the instability problem for operator perturbations. One might wonder whether operators which are "close" (in some sense) also have spectra which are "close". Unfortunately, this is in general not true. Even in finite dimensions this breaks down, as the following example shows.

Example 2.14 ([28]). Let $\mathcal{X} = \mathbb{R}^n$ and let

$$M = \begin{bmatrix} 0 & 1 & & \\ & \ddots & \ddots & \\ & & & 1 \\ & & & 0 \end{bmatrix}. \quad (2.22)$$

M is nilpotent so $\sigma(M) = \{0\}$. However, for an arbitrarily small $\epsilon > 0$, the perturbation

$$M + E = \begin{bmatrix} 0 & 1 & & \\ & \ddots & \ddots & \\ & & & 1 \\ \epsilon & & & 0 \end{bmatrix}. \quad (2.23)$$

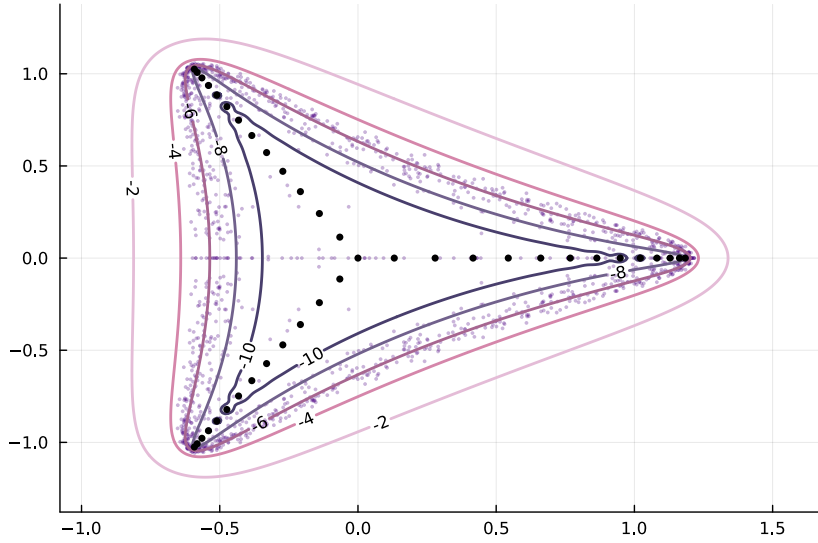


Figure 2.3: Pseudospectra for the 40×40 Toeplitz matrix T with 0 on the main diagonal, 1 on the first upper off-diagonal, and $1/4$ on the second lower off-diagonal. Contour lines show the boundary of the ϵ -pseudospectrum for $\epsilon = 10^{-2}, 10^{-4}, 10^{-6}, 10^{-8}, 10^{-10}$. Black: Spectrum of T . Purple: Spectra of $T + E$ for 40 randomly sampled perturbations E with $\|E\| < 10^{-4}$.

has characteristic polynomial $(-\lambda)^n - (-1)^n \epsilon$ so that $\sigma(M+E) = \{\lambda \in \mathbb{C} \mid \lambda^n = \epsilon\}$. For growing n , $\sigma(M+E)$ comes asymptotically close to filling the unit circle.

2.3.1 Definitions of the Pseudospectrum

Definition 2.15. Let $M : D(M) \rightarrow \mathcal{X}$ be a closed linear operator. The ϵ -pseudospectrum of M is the smallest set in \mathbb{C} which contains the spectrum of all perturbations of M with norm less than ϵ .³

$$\sigma_\epsilon(M) = \bigcup_{\|E\| < \epsilon} \sigma(M+E). \quad (2.24)$$

Theorem 2.16. We have the following equivalent formulation of the pseudospectrum:

$$\sigma_\epsilon(M) = \left\{ \lambda \in \mathbb{C} \mid \|(M - \lambda I)^{-1}\| > \frac{1}{\epsilon} \right\} \quad (2.25)$$

where we use the convention that $\|(M - \lambda I)^{-1}\| = \infty$ if $M - \lambda I$ is not invertible.

Remark. While this result is practically pseudospectrum folklore, a correct proof in the general case of closed linear operators on Banach spaces is difficult to find. Virtually all sources which cite this result, cite an unpublished

³Some authors will define the pseudospectrum with " \leq " instead of " $<$ ". This makes $\sigma_\epsilon(M)$ a closed set, but breaks theorem 2.16.

technical report by Chaitin-Chatelin and Harrabi [7]. The following proof is based on [5] and extended slightly from bounded operators to closed (potentially) unbounded operators.

Proof. We prove " \subset " by contraposition: assume $\|(M - \lambda I)^{-1}\| > \frac{1}{\epsilon}$ and let $\|E\| < \epsilon$. Then $\|(M - \lambda I)^{-1}E\| < 1$ and hence $I + (M - \lambda I)^{-1}E$ is invertible. This implies

$$M - \lambda I + E = (M - \lambda I)(I + (M - \lambda I)^{-1}E) \quad (2.26)$$

is invertible.

Conversely, we prove " \supset " by showing there exists an operator E with $\|E\| < \epsilon$ such that $M - \lambda I + E$ is not invertible. Since $\|(M - \lambda I)^{-1}\| > \frac{1}{\epsilon}$ there exists a $u \in \mathcal{X}$ with $\|u\| = 1$ and $(M - \lambda I)^{-1}u = v \in D(M)$ with $\|v\| = \frac{1}{\delta} > \frac{1}{\epsilon}$.⁴ The Hahn-Banach theorem provides a $v^* \in \mathcal{X}^*$ with $\|v^*\| = 1$ and $v^*v = \|v\| = \frac{1}{\delta}$. Set $E = -\delta uv^*$. Then $\|E\| = \delta < \epsilon$ and

$$Ev = -\delta uv^*v = -u = -(M - \lambda I)(M - \lambda I)^{-1}u = -(M - \lambda I)v. \quad (2.27)$$

Rearranging yields $(M + E - \lambda I)v = 0$. \square

The proof of the above theorem also shows that one can consider only rank-one perturbations in 2.24:

Corollary 2.17. *We can restrict 2.24 to*

$$\sigma_\epsilon(M) = \bigcup_{\substack{\|E\| < \epsilon \\ \text{rank } E=1}} \sigma(M + E). \quad (2.28)$$

The following formulation of the pseudospectrum in the Hilbert space case will be the main tool we use in the section on numerical methods.

Definition 2.18. *The function*

$$\sigma_{\inf}(M) = \inf_{\|x\|=1} \|Mx\| \quad (2.29)$$

is known as the injection modulus.

Lemma 2.19. *Let $M : D(M) \rightarrow \mathcal{X}$ be a closed linear operator on a Hilbert space. If $\lambda \in \rho(M)$ then*

$$\sigma_{\inf}(M - \lambda I) = \sigma_{\inf}(M^* - \bar{\lambda}I), \quad (2.30)$$

but this is not necessarily true if $\lambda \in \sigma(M)$.

⁴At this point we require the strict inequality. Otherwise, the existence of such a pair u , v is not guaranteed.

Proof. 2.30 for $\lambda \in \rho(M)$ follows from the fact that for bounded operators A we have $\|A\| = \|A^*\|$, applied to $A = (M - \lambda I)^{-1}$. To see that 2.30 does not hold for $\lambda \in \sigma(M)$, consider again the right shift from example 2.8. Clearly $\|Rx\| = \|x\|$ so R is bounded from below but 0 is part of the spectrum. \square

Theorem 2.20. *For a Hilbert space operator M ,*

$$\frac{1}{\|(M - \lambda I)^{-1}\|} = \min \{\sigma_{\inf}(M - \lambda I), \sigma_{\inf}(M^* - \bar{\lambda}I)\}. \quad (2.31)$$

where we use the convention that $1/\|(M - \lambda I)^{-1}\| = 0$ when $\lambda \in \sigma(M)$.

Proof. When $\lambda \in \sigma_p(M)$, then obviously $\sigma_{\inf}(M - \lambda I) = 0$. Due to theorem 2.9 part 2, $\lambda \in \sigma_r(M)$ has $\sigma_{\inf}(M^* - \bar{\lambda}I) = 0$. Finally, let $\lambda \in \sigma_c(M)$ so $M - \lambda I$ is injective. Assume $\sigma_{\inf}(M - \lambda I) > 0$. Then $(M - \lambda I)^{-1} : \text{ran}(M - \lambda I) \rightarrow D(M)$ is bounded. But since $\text{ran}(M - \lambda I) \subset \mathcal{X}$ is dense, $(M - \lambda I)^{-1}$ has a unique bounded extension to \mathcal{X} , a contradiction. \square

Corollary 2.21. *In the Hilbert space setting, the pseudospectrum can be formulated as:*

$$\begin{aligned} \sigma_\epsilon(M) = \{&\lambda \in \mathbb{C} \mid \exists u \in \mathcal{X} : \|u\| = 1 \text{ and either} \\ &\|(M - \lambda I)u\| < \epsilon \text{ or } \|(M^* - \bar{\lambda}I)u\| < \epsilon\}. \end{aligned} \quad (2.32)$$

In the general Banach space setting,

$$\sigma_\epsilon(M) = \sigma_r(M) \cup \{\lambda \in \mathbb{C} \mid \exists u \in \mathcal{X} : \|u\| = 1, \|(M - \lambda I)u\| < \epsilon\}. \quad (2.33)$$

The residual spectrum causes many common and unintuitive issues in spectral theory. In the study of pseudospectra, this issue is alleviated in one of three ways: (1): consider only classes of operators which have no residual spectrum (e.g. finite-dimensional or compact operators), (2): compute a slightly different object known as the *approximate-point spectrum* (see below), (3): ignore the problem entirely and write proofs which are all slightly incorrect.

Definition 2.22. *The approximate-point pseudospectrum is the set of points for which there exists an ϵ -approximate pseudoeigenvector*

$$\sigma_{ap,\epsilon}(M) = \{\lambda \in \mathbb{C} \mid \exists u \in \mathcal{X} : \|u\| = 1, \|(M - \lambda I)u\| < \epsilon\}. \quad (2.34)$$

The $\epsilon \rightarrow 0$ limit of such sets is the approximate-point spectrum

$$\sigma_{ap}(M) = \bigcap_{\epsilon > 0} \sigma_{ap,\epsilon}(M) \quad (2.35)$$

$$= \left\{ \lambda \in \mathbb{C} \mid \exists (u_k)_k : \|u_k\| = 1 \forall k, \lim_{k \rightarrow \infty} \|(M - \lambda I)u_k\| = 0 \right\}. \quad (2.36)$$

2.3.2 Properties

To gain some intuition for the pseudospectrum, we derive some properties for specific types of operators.

Definition 2.23. An operator M on a Hilbert space is called *normal* if $M^*M = MM^*$. Special classes of normal operator include unitary operators ($M^* = M^{-1}$) and self-adjoint operators ($M^* = M$).

Proposition 2.24. For a normal operator M , $\sigma_r(M) = \emptyset$.

Proof. Let $\lambda \in \sigma(M)$, $A = M - \lambda I$. If λ is not an eigenvalue then $\ker A = \{0\}$ and

$$\{0\} = \ker A = \ker A^* = (\text{ran } A)^\perp \quad (2.37)$$

where for the second equality we used the normality. Hence $\text{ran } A$ is dense. \square

Lemma 2.25. For a closed linear operator M we have

$$\text{dist}(\lambda, \sigma(M)) \geq \frac{1}{\|(M - \lambda I)^{-1}\|}. \quad (2.38)$$

Moreover, if M is a normal operator on a Hilbert space, then we have equality.

Proof. Let $\eta \in \sigma(M)$. Denote $A = M - \lambda I$, $B = M - \eta I$. Then A is invertible and

$$B = A - (A - B) = A(I - A^{-1}(A - B)). \quad (2.39)$$

Now $\|A^{-1}(A - B)\| \leq \|A^{-1}\| |\lambda - \eta|$ so if $|\lambda - \eta| < \frac{1}{\|B^{-1}\|}$ then the right hand side of 2.39 is invertible, a contradiction to $\eta \in \sigma(M)$.

To prove equality in the case of normal operators requires some heavy machinery from operator theory, namely:

1. Every normal operator is unitarily similar to a multiplication operator on some semi-finite measure space (i.e. there exists a unitary U such that $M = U^{-1}M_aU$ where $(M_a f)(x) = a(x)f(x)$ is a multiplication operator).
2. For multiplication operators, equation 2.38 holds with equality.

These results can be found in many sources e.g. [27]. \square

Theorem 2.26. We have

1. $\sigma_\delta(M) \subset \sigma_\epsilon(M)$ whenever $\delta \leq \epsilon$,
2. $\bigcap_{\epsilon > 0} \sigma_\epsilon(M) = \sigma(M)$,
3. $\sigma(M) + B_\epsilon \subset \sigma_\epsilon(M)$, where B_ϵ is the ball with radius ϵ centered at 0 and + refers to pointwise summation $C + D = \{x + y \mid x \in C, y \in D\}$.
4. When M is normal, $\sigma(M) + B_\epsilon = \sigma_\epsilon(M)$.

Remark. Theorem 2.26 effectively says that the Pseudospectra are nested sets which grow *at least* as quickly as ϵ -balls around the spectrum.

Proof. 1 and 2 are consequences of the representation 2.24 of the pseudospectrum. 3 and 4 are consequences of lemma 2.25. \square

Theorem 2.27. *The function which maps $(\epsilon, M) \mapsto \sigma_\epsilon(M)$ which sends an $\epsilon > 0$ and a bounded M acting on a Hilbert space \mathcal{X} to the set $\sigma_\epsilon(M)$ is continuous using the metric*

$$d((\epsilon_1, M_1), (\epsilon_2, M_2)) = |\epsilon_1 - \epsilon_2| + \|M_1 - M_2\| \quad (2.40)$$

in the domain and the Haussdorff metric in the codomain.

Remark. 1. The idea for the proof is taken from [11], though it originally included two errors: it does not take into account residual spectrum, and makes a bound which is unfortunately not correct. These issues can be lifted in the Hilbert space setting, so that the theorem is still correct as it is stated in [11].

2. If one replaces $\sigma_\epsilon(M)$ with $\sigma_{ap,\epsilon}(M)$ in theorem 2.27, then the proof in [11] is correct and even works for general Banach spaces. To the best of this author's knowledge, there is no published correct proof for the general Banach space setting with $\sigma_\epsilon(M)$, despite it being considered common knowledge in the study of pseudospectra.

Proof. Let (M, ϵ) and (M', ϵ') be such that $d((M, \epsilon), (M', \epsilon')) < \delta$ for some $0 < \delta < \epsilon/2$. Without loss of generality let $\epsilon \leq \epsilon'$.

Let $\lambda \in \sigma_{\epsilon'}(M')$. By 2.32 there exists a normalized $v \in \mathcal{X}$ such that either $\|(M' - \lambda I)v\| < \epsilon'$ or $\|(M'^* - \bar{\lambda}I)v\| < \epsilon'$. Assume the former is true. It follows

$$\|(M - \lambda I)v\| \leq \|(M - M')v\| + \|(M' - \lambda I)v\| < \delta - |\epsilon - \epsilon'| + \epsilon' \leq \delta + \epsilon \quad (2.41)$$

where for the last inequality we used that $\epsilon \geq \epsilon' - |\epsilon' - \epsilon|$. By 2.32, $\lambda \in \sigma_{\epsilon+\delta}(M)$ and hence $\sigma_{\epsilon'}(M') \subset \sigma_{\epsilon+\delta}(M)$.

For the case that $\|(M'^* - \bar{\lambda}I)v\| < \epsilon'$, equation 2.41 can be done exactly the same with $\|(M^* - \bar{\lambda}I)v\|$ on the left hand side.

Now let $\lambda \in \sigma_{\epsilon-\delta}(M)$. Again this implies there exists a normalized $v \in \mathcal{X}$ such that either $\|(M - \lambda I)v\| < \epsilon - \delta$ or $\|(M^* - \bar{\lambda}I)v\| < \epsilon - \delta$. Assume again the former is true. Then

$$\|(M' - \lambda I)v\| \leq \|(M' - M)v\| + \|(M - \lambda I)v\| < \delta + \epsilon - \delta \leq \epsilon' \quad (2.42)$$

and hence $\lambda \in \sigma_{\epsilon'}(M')$ so that $\sigma_{\epsilon-\delta}(M) \subset \sigma_{\epsilon'}(M')$ (again the adjoint case can be done exactly the same with adjoints on the left hand side of the equation).

We now have $\sigma_{\epsilon-\delta}(M) \subset \sigma_{\epsilon'}(M') \subset \sigma_{\epsilon+\delta}(M)$ which implies for the Haussdorff distance between $\sigma_\epsilon(M)$ and $\sigma_{\epsilon'}(M')$,

$$\mathcal{H}(\sigma_\epsilon(M), \sigma_{\epsilon'}(M')) \quad (2.43)$$

$$\leq \max \{ \mathcal{H}(\sigma_\epsilon(M), \sigma_{\epsilon-\delta}(M)), \mathcal{H}(\sigma_\epsilon(M), \sigma_{\epsilon+\delta}(M)) \} \quad (2.44)$$

$$\leq \mathcal{H}(\sigma_{\epsilon-\delta}(M), \sigma_{\epsilon+\delta}(M)) \quad (2.45)$$

so we must investigate the difference between $\sigma_{\epsilon-\delta}(M)$ and $\sigma_{\epsilon+\delta}(M)$. But

$$\sigma_{\epsilon+\delta}(M) \setminus \sigma_{\epsilon-\delta}(M) = \left\{ \lambda \in \mathbb{C} \mid \frac{1}{\epsilon + \delta} < \| (M - \lambda I)^{-1} \| < \frac{1}{\epsilon - \delta} \right\} \quad (2.46)$$

which is just a difference of sublevel sets for the continuous function $\lambda \mapsto \| (M - \lambda I)^{-1} \|$. Hence 2.46 collapses continuously to \emptyset as $\delta \rightarrow 0$, which implies 2.45 converges to 0 as $\delta \rightarrow 0$. \square

We conclude the section on mathematical background by examining the interaction between an operator and finite rank approximations of it. The methods we will describe in the following section are special types of *finite-section methods*.

Theorem 2.28. *Let M be a closed linear operator and $(\Pi_n : \mathcal{X} \rightarrow V_n)_n$ be a collection of projections onto finite-dimensional subspaces V_n which converge pointwise to the identity. Let further (λ, c) be an ϵ -pseudoeigenpair of $\Pi_n M \Pi_n$. Then for every $\delta > 0$ there exists an $N = N(\delta, c)$ such that $\lambda \in \sigma_{\epsilon+\delta}(M)$ whenever $n > N$.*

However, this does not necessarily imply $\sigma_\epsilon(\Pi_n M \Pi_n) \rightarrow \sigma_\epsilon(M)$ in the Haussdorff metric.

Proof. Let N be such that off-diagonal action of $(M - \lambda I)$ on c is bounded by δ , i.e. $\| (I - \Pi_N)(M - \lambda I)\Pi_N c \| < \delta$. Now the claim follows from the triangle inequality since

$$(M - \lambda I)c = (\Pi_N M \Pi_N - \lambda I)c + (I - \Pi_N)(M - \lambda I)\Pi_N c \quad (2.47)$$

and (by definition) $c = \Pi_N c$.

For the second claim of the theorem consider the *two-sided* left shift operator $L : \ell^2 \rightarrow \ell^2$ and let

$$\Pi_n : (\dots, a_{-1}, a_0, a_1, \dots) \mapsto (\dots, 0, 0, a_{-n}, \dots, a_{-1}, a_0, a_1, \dots, a_n, 0, 0, \dots). \quad (2.48)$$

Then L is unitary and has spectrum on the (complex) unit circle \mathbb{T} , so $\sigma_\epsilon(L) = \mathbb{T} + B_\epsilon$. However, $\Pi_n L \Pi_n$ is nilpotent so $\sigma_\epsilon(\Pi_n L \Pi_n)$ always contains 0, which is not in $\mathbb{T} + B_\epsilon$ for any $\epsilon < 1$. \square

With an understanding of the spectral properties of Koopman and Perron-Frobenius operators as well as the pseudospectrum, we are prepared to apply pseudospectral methods to some of the most common Koopman approximation methods, known under the umbrella term *dynamic mode decomposition*.

3 Numerical Methods

3.1 Petrov-Galerkin Methods

The original Ritz-Galerkin method is described as follows: we are given a PDE problem in its *weak formulation*:

$$\text{find } u \in \mathcal{X} \text{ such that } q(v, u) = \langle f, v \rangle \quad \forall v \in \mathcal{W} \quad (3.1)$$

where q is some elliptic sesquilinear form, $f \in \mathcal{X}$ given, $\langle \cdot, \cdot \rangle$ some inner product, and \mathcal{W} some *test set*. The form q is typically derived from some minimization problem for a functional representing energy.

The idea behind the Ritz-Galerkin method is to *solve 3.1 on a finite-dimensional subspace*: let $\mathcal{W} = \text{span}\{\psi_1, \dots, \psi_N\}$ be q -linearly independent.

Then writing

$$\Psi(x) = [\psi_1(x) \mid \dots \mid \psi_N(x)], \quad (3.2)$$

we make the approximation $u \approx \Psi c_u$ and have $v = \Psi c_v$ for $c_u, c_v \in \mathbb{C}^N$. Now 3.1 reduces to

$$\text{find } c_u \in \mathbb{C}^N \text{ such that } q(\Psi c_v, \Psi c_u) = \langle f, \Psi c_v \rangle \quad \forall c_v \in \mathbb{C}^N. \quad (3.3)$$

One quickly verifies that c_u is the unique solution to the matrix equation $Ax = b$ with

$$A_{ij} = q(\Psi e_i, \Psi e_j) = q(\psi_i, \psi_j), \quad b_i = \langle f, \Psi e_i \rangle = \langle f, \psi_i \rangle. \quad (3.4)$$

where $e_i \in \mathbb{C}^N$ is the i -th standard unit vector. A is known as the *stiffness matrix*.

One can extend the Ritz-Galerkin formulation by allowing the test space to differ from the basis space: keep $u \approx \Psi c_u$ but let $\mathcal{W} = \text{span}\{\psi_1^*, \dots, \psi_M^*\}$, then A and b become

$$A_{ij} = q(\psi_i^*, \psi_j), \quad b_i = \langle f, \psi_i^* \rangle. \quad (3.5)$$

In the regime $M > N$ this equation is *overdetermined* so it is solved in a least squares sense

$$\|Ax - b\|_2^2 = \min_{x \in \mathbb{C}^N} \|Ax - b\|_2^2 \quad (3.6)$$

where $\|\cdot\|_2$ is the vector ℓ^2 norm. This is known as the Petrov-Galerkin method.

One can extend the method further by asking that multiple solutions for multiple right hand sides $(f_j)_{j=1}^N$ are computed simultaneously, that is

$$\|AX - B\|_F^2 = \min_{X \in \mathbb{C}^{N \times N}} !, \quad B_{ij} = \langle f_j, \psi_i^* \rangle \quad (3.7)$$

where $\|\cdot\|_F$ denotes the Frobenius norm.

Numerically, 3.7 can be solved using the Moore-Penrose inverse

$$X = A^\dagger B. \quad (3.8)$$

An exercise in matrix calculus shows that the solution can also be written in the form

$$X = (A^* A)^{-1} A^* B. \quad (3.9)$$

Both forms will prove to be useful later.

3.2 Extended Dynamic Mode Decomposition (EDMD)

3.2.1 The Galerkin Ansatz

We apply the Petrov-Galerkin Ansatz to obtain a matrix approximation K for $\mathcal{K}|_{\mathcal{X}}$. Let $q(\cdot, \cdot) = \langle \cdot, \cdot \rangle$ and consider a linearly independent family of functions $\{\psi_1, \dots, \psi_N\} \subset \mathcal{X}$. Take delta distributions, that is $\langle \delta_x, \psi \rangle = \psi(x)$, for the test function(als): let $(w_i, x_i)_{i=1}^M$ represent a quadrature scheme and set $\psi_i^* = \sqrt{w_i} \delta_{x_i}$.

We then solve the Galerkin equation 3.7 for $f_j = \mathcal{K}\psi_j$:

$$\left\| \sqrt{W} \Psi_X K - \sqrt{W} \Psi_Y \right\|_F^2 = \min_{K \in \mathbb{C}^{N \times N}} ! \quad (3.10)$$

with $W = \text{diag}(w_1, \dots, w_M)$ and

$$(\Psi_X)_{ij} = \langle \delta_{x_i}, \psi_j \rangle = \psi_j(x_i), \quad (\Psi_Y)_{ij} = \langle \delta_{x_i}, \mathcal{K}\psi_j \rangle = \psi_j(S(x_i)). \quad (3.11)$$

This results in the *EDMD matrix*

$$K = \Psi_X^\dagger \Psi_Y = (\Psi_X^* W \Psi_X)^{-1} (\Psi_X^* W \Psi_Y). \quad (3.12)$$

Inverting Ψ_X involves computing the Moore-Penrose inverse of an $N \times M$ matrix, whereas inverting $\Psi_X^* \Psi_X$ involves computing the inverse of a symmetric $N \times N$ matrix. Depending on the relationship between M and N in the particular usecase, either formulation might be cheaper.

Another look at the second formulation of the EDMD matrix shows that

$$G_{ij} := (\Psi_X^* W \Psi_X)_{ij} = \sum_{k=1}^M w_k \overline{\psi_i(x_k)} \psi_j(x_k) \xrightarrow{M \rightarrow \infty} \langle \psi_i, \psi_j \rangle =: \mathbb{G}_{ij}, \quad (3.13)$$

$$A_{ij} := (\Psi_X^* W \Psi_Y)_{ij} = \sum_{k=1}^M w_k \overline{\psi_i(x_k)} \psi_j(S(x_k)) \xrightarrow{M \rightarrow \infty} \langle \psi_i, \mathcal{K} \psi_j \rangle =: \mathbb{A}_{ij}, \quad (3.14)$$

which can be computed with constant memory requirement.

3.2.2 Functional Minimization

We could have arrived at equation 3.10 completely differently: equation 3.10 is precisely a quadrature approximation of the functional least squares minimization:

$$\|\Psi K - \mathcal{K} \Psi\|_{\mathcal{X}^{1 \times N}}^2 = \min_{K \in \mathbb{C}^{N \times N}} ! \quad (3.15)$$

where $\mathcal{K} \Psi$ is understood elementwise and $\mathcal{X}^{1 \times N}$ is the space of (row) vector-valued functions with each component in \mathcal{X}

$$\|[f_1 | \dots | f_N]\|_{\mathcal{X}^{1 \times N}}^2 = \|f_1\|_{\mathcal{X}}^2 + \dots + \|f_N\|_{\mathcal{X}}^2. \quad (3.16)$$

Let us investigate $\Psi : \mathbb{C}^N \rightarrow \mathcal{X}$ a bit closer. Decompose the Hilbert space \mathcal{X} into

$$\mathcal{X} = \text{span } \{\psi_j\}_{j=1}^N \oplus \mathcal{V}, \quad \mathcal{V} = \left(\{\psi_j\}_{j=1}^N \right)^\perp \quad (3.17)$$

and let $\{\psi_j\}_{j=N+1}^\infty$ be a basis of \mathcal{V} .

A short calculation using the orthogonality of $\{\psi_j\}_{j=1}^N$ and $\{\psi_j\}_{j=N+1}^\infty$ shows that for $\phi \in \mathcal{X}$,

$$\langle \phi, \Psi c \rangle = \sum_{j=1}^N \langle \phi, \psi_j \rangle c_j. \quad (3.18)$$

Hence the adjoint quasi-matrix $\Psi^* : \mathcal{X} \rightarrow \mathbb{C}^N$ acts as

$$\Psi^* \phi = \begin{pmatrix} \langle \phi, \psi_1 \rangle \\ \vdots \\ \langle \phi, \psi_N \rangle \end{pmatrix}. \quad (3.19)$$

Lemma 3.1. *For an arbitrary basis $\{\psi_j\}_{j=1}^N$, the orthogonal projector Π onto the space spanned by the basis is*

$$\Pi = \Psi(\Psi^* \Psi)^{-1} \Psi^*. \quad (3.20)$$

Proof. The solution of a linear least squares problem $\|Ax - b\| = \min!$ is the result of orthogonally projecting b onto the range of A , that is, $Ax = \Pi b$. From equation 3.9 we know $x = (A^* A)^{-1} A^* b$. Therefore $\Pi b = Ax = A(A^* A)^{-1} A^* b$. Since this holds for arbitrary b , the result is proven. \square

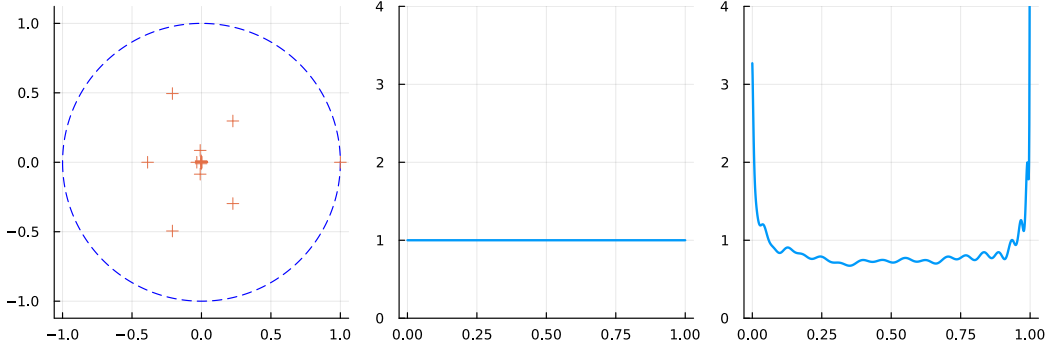


Figure 3.1: Algorithm 1 applied to the quadratic map (c.f. figure 2.1) performed with $M = 100$ Gauß-Legendre quadrature nodes and weights, and $N = 40$ Legendre polynomials transplanted to the interval $[0, 1]$. Left: spectrum of K . Middle: (normalized) eigenfunction of K for the eigenvalue $\lambda = 1$. Right: (normalized) eigenfunction of L for the eigenvalue $\lambda = 1$. Compare with figure 2.2.

Using equation 3.9 we see that in the infinite-data limit $M \rightarrow \infty$, K has the form

$$K = (\Psi^* \Psi)^{-1} \Psi^* (\mathcal{K} \Psi) \quad (3.21)$$

Inserting the definitions of Ψ and Ψ^* yields $K = \mathbb{G}^{-1} \mathbb{A}$ exactly as in equations 3.13 and 3.14.

If we view the result of applying K as in equation 3.21 to a vector c as an object in \mathcal{X} , that is, $\Psi K c$, we see that

$$\Psi K c = \Psi(\Psi^* \Psi)^{-1} \Psi^* (\mathcal{K} \Psi) c = \Pi \mathcal{K} \Psi c = \Pi \mathcal{K} \Pi \Psi c. \quad (3.22)$$

Since this holds for arbitrary c we have proven that (when viewed as an operator on \mathcal{X}) K is precisely the action of $P \mathcal{K} P$, the finite section of \mathcal{K} over $\text{span}\{\psi_j\}_{j=1}^N$. In this way, EDMD can just as well be viewed as a finite section method.

Algorithm 1 Extended Dynamic Mode Decomposition (EDMD)

Require: Dictionary $\{\psi_j\}_{j=1}^N$, data points and weights $\{(w_i, x_i)\}_{i=1}^M$

- 1: Construct G , A as in 3.13, 3.14
 - 2: Set $K = G^{-1} A$ (or $L = G^{-1} A^*$)
 - 3: Compute an eigendecomposition $KV = V\Lambda$ (or $LV = V\Lambda$)
 - 4: **return** Eigenvalues and eigenvectors Λ , V
-

3.2.3 EDMD for the Perron-Frobenius Operator

From equation 3.21, and noting the form of \mathbb{A} ,

$$\langle \psi_i, \mathcal{L} \psi_j \rangle = \langle \mathcal{K} \psi_i, \psi_j \rangle = \overline{\langle \psi_j, \mathcal{K} \psi_i \rangle} = \overline{\mathbb{A}_{ji}} \quad (3.23)$$

yields an equivalent Galerkin method for \mathcal{L} :

$$L = (\Psi^* \Psi)^{-1} \Psi^* (\mathcal{L} \Psi) = \mathbb{G}^{-1} \mathbb{A}^* \quad (3.24)$$

or the finite analogue:

$$L = G^{-1} A^*. \quad (3.25)$$

3.3 Residual EDMD (ResDMD)

3.3.1 Validation of Koopman Eigenpairs

The formulation 3.22 shows that K (when viewed as a operator on \mathcal{X}) converges weakly to \mathcal{K} . However, from example 2.14 we know that the spectrum is already unstable for operators which are close in the *strong* operator topology, let alone in the *weak* topology. It is therefore entirely unclear *a priori* that the eigenvalues and eigenvectors of K actually represent eigenvalues and eigenfunctions of \mathcal{K} .

In the Perron-Frobenius operator community, a common solution to the mentioned issue is *stochastic smoothing*. Instead of considering a deterministic dynamical system generated by S , one consider a stochastic system: $x \in \Omega$ is assigned a *distribution* of possible image points instead of being assigned to the point $S(x)$. The resulting Markov process has an associated (stochastic) Perron-Frobenius operator which (under some conditions on the type of stochastic smoothing) is Hilbert-Schmidt on $L^2(\Omega)$. This way, the finite sections converge strongly to the (stochastic) Perron-Frobenius and (since it is Hilbert-Schmidt) so do the eigenvalues [12].

We take a different approach using the theory of pseudospectra. We wish to know which of our eigenvalues are *spurious*, that is, caused by the reduction to a finite section, and which eigenvalues are accurate. To determine this, we consider equation 2.32: if a sequence $(\lambda_N, c_N)_N$ of (normalized) eigenpairs for $K = K(\{\psi_j\}_{j=1}^N)$ converges to a true $\lambda \in \sigma(\mathcal{K})$ then we must have

$$\lim_{N \rightarrow \infty} \|(\mathcal{K} - \lambda_N I)\Psi c_N\|_{\mathcal{X}}^2 = 0 \quad (3.26)$$

(where $\Psi = \Psi_N$ is as in 3.2) or

$$\lim_{N \rightarrow \infty} \|(\mathcal{L} - \lambda_N I)\Psi c_N\|_{\mathcal{X}}^2 = 0. \quad (3.27)$$

Conversely, if neither of these tend to 0 as N grows, then we can rule out λ_N as a candidate eigenvalue.

From section 3.2.2 we know that the Galerkin equation 3.10 is a quadrature approximation of equation 3.15. Similarly, the *regression error*

$$\text{res}_{N,M}(\lambda_N, c_N) := \left\| \sqrt{W}(\Psi_Y - \lambda_N \Psi_X)c_N \right\|_2^2 \quad (3.28)$$

is precisely a quadrature approximation of equation 3.26.

Theorem 3.2. Let λ and $g = \Psi c$ be a candidate eigenpair for \mathcal{K} . Then

$$\lim_{M \rightarrow \infty} \text{res}_{N,M}(\lambda, c) = \|(\mathcal{K} - \lambda I)g\|_{\mathcal{X}}^2 \quad (3.29)$$

Proof. Denote $J = \Psi_Y^* W \Psi_Y$ and observe that

$$\lim_{M \rightarrow \infty} J_{ij} = \langle \mathcal{K}\psi_i, \mathcal{K}\psi_j \rangle =: \mathbb{J}_{ij}. \quad (3.30)$$

Consider the action of Ψ on standard unit vectors:

$$\langle \Psi e_i, \Psi e_j \rangle = \langle \psi_i, \psi_j \rangle = \mathbb{G}_{ij} = e_i^* \mathbb{G} e_j. \quad (3.31)$$

Analogously $e_i^* \mathbb{A} e_j = \langle \psi_i, \mathcal{K}\psi_j \rangle$, $e_i^* \mathbb{J} e_j = \langle \mathcal{K}\psi_i, \mathcal{K}\psi_j \rangle$. Sesquilinearity of $\langle \cdot, \cdot \rangle$ yields

$$\langle g, g \rangle = c^* \mathbb{G} c, \quad \langle g, \mathcal{K}g \rangle = c^* \mathbb{A} c, \quad \langle \mathcal{K}g, \mathcal{K}g \rangle = c^* \mathbb{J} c. \quad (3.32)$$

The proof is now simply a calculation. Indeed,

$$\begin{aligned} & \left\| \sqrt{W} (\Psi_Y - \lambda \Psi_X) c \right\|_2^2 \\ &= ((\Psi_Y - \lambda \Psi_X) c)^* W ((\Psi_Y - \lambda \Psi_X) c) \\ &= c^* (\Psi_Y^* W \Psi_Y - \bar{\lambda} \Psi_X^* W \Psi_Y - \lambda \Psi_Y^* W \Psi_X + |\lambda|^2 \Psi_X^* W \Psi_X) c \\ &= c^* J c - \bar{\lambda} c^* A c - \lambda c^* A^* c + |\lambda|^2 c^* G c. \end{aligned} \quad (3.33)$$

Taking the infinite-data limit,

$$\begin{aligned} & \lim_{M \rightarrow \infty} \left\| \sqrt{W} (\Psi_Y - \lambda \Psi_X) c \right\|_2^2 \\ &= c^* \mathbb{J} c - \bar{\lambda} c^* \mathbb{A} c - \lambda c^* \mathbb{A}^* c + |\lambda|^2 c^* \mathbb{G} c \\ &= \langle \mathcal{K}g, \mathcal{K}g \rangle - \bar{\lambda} \langle g, \mathcal{K}g \rangle - \bar{\lambda} \langle \mathcal{K}g, g \rangle + |\lambda|^2 \langle g, g \rangle \\ &= \langle (\mathcal{K} - \lambda I) g, (\mathcal{K} - \lambda I) g \rangle \\ &= \|(\mathcal{K} - \lambda I) g\|_{\mathcal{X}}^2. \end{aligned} \quad (3.34)$$

□

From the proof we also directly see the following corollaries.

Definition 3.3. Let $M : \mathcal{X} \supset D(M) \rightarrow \mathcal{Y}$ be a closed linear operator and $V \subset \mathcal{X}$. We say that V forms a core of M if the closure⁵ of $M|_V$ if M .

⁵A linear operator $N : D(N) \rightarrow \mathcal{Y}$ which is *not* closed might only be so because the domain $D(N)$ might not be "large enough". If there exists an extension (i.e. $\bar{N} : D(\bar{N}) \rightarrow \mathcal{Y}$, $D(N) \subset D(\bar{N})$, $\bar{N}|_{D(N)} = N$) which is closed, then N is *closable* and the smallest such \bar{N} is called the *closure* of N .

Corollary 3.4. Let $\lambda \in \mathbb{C}$, define

$$\text{res}_{N,M}(\lambda) := \min_{c^* G c = 1} \left\| \sqrt{W} (\Psi_Y - \lambda \Psi_X) c \right\|_2. \quad (3.35)$$

Then

$$\lim_{M \rightarrow \infty} \text{res}_{N,M}(\lambda) = \min_{\substack{g \in \text{span}\{\psi_1, \dots, \psi_N\} \\ \|g\|=1}} \|(\mathcal{K} - \lambda I)g\|_{\mathcal{X}}. \quad (3.36)$$

In particular this corollary implies that if we calculate some candidate eigenpairs, compute $\text{res}_{N,M}$ for each one, and throw out eigenpairs which do not satisfy a threshhold $\text{res}_{M,N}(\lambda, c) < \epsilon$, then the remaining candidate eignpairs really are close to eigenpairs of \mathcal{K} . This process is summarized in algorithm 2.

Corollary 3.5. Let $\Lambda_M(\epsilon)$ denote the set of eigenvalues returned by algorithm 2. Then

$$\limsup_{M \rightarrow \infty} \max_{\lambda \in \Lambda_M(\epsilon)} \|(\mathcal{K} - \lambda I)^{-1}\|^{-1} \leq \epsilon. \quad (3.37)$$

Finally, theorem 3.2 also provides a method to compute the ϵ -approximate point pseudospectrum of \mathcal{K} , summarized in algorithm 3.

Corollary 3.6. Assume $\text{span}\{\psi_j\}_{j=1}^\infty$ forms a core of \mathcal{K} . Then

$$\lim_{N \rightarrow \infty} \lim_{M \rightarrow \infty} \text{res}_{N,M}(\lambda) = \sigma_{\inf}(\mathcal{K} - \lambda I). \quad (3.38)$$

Moreover the outer limit $N \rightarrow \infty$ is monotonically decreasing so that

$$\sigma_{ap,\epsilon}(\mathcal{K}) = \bigcap_{N>0} \left\{ \lambda \in \mathbb{C} \mid \lim_{M \rightarrow \infty} \text{res}_{N,M}(\lambda) < \epsilon \right\}. \quad (3.39)$$

Proof. From 3.36 it is clear that $\lim_{M \rightarrow \infty} \text{res}_{N,M}(\lambda) \geq \sigma_{\inf}(\mathcal{K} - \lambda I)$ and that $\text{res}_{N,M}$ is decreasing with N . Let $\delta > 0$ be arbitrary and $g \in \mathcal{X}$ be such that $\|g\| = 1$ and $\|(\mathcal{K} - \lambda I)g\| < \sigma_{\inf}(\mathcal{K} - \lambda I) + \delta$. Since $\text{span}\{\psi_j\}_{j=1}^\infty$ forms a core of \mathcal{K} , we can find an N and $\hat{g} \in \text{span}\{\psi_j\}_{j=1}^N$ such that $\|g - \hat{g}\| < \delta$ and $\|(\mathcal{K} - \lambda I)\hat{g}\| < \|(\mathcal{K} - \lambda I)g\| + \delta$. This implies $\|\hat{g}\| > 1 - \delta$ and $\|(\mathcal{K} - \lambda I)\hat{g}\| < (\sigma_{\inf}(\mathcal{K} - \lambda I) + 2\epsilon)/(1 - \epsilon)$. Since this holds for all $\epsilon > 0$, the claim is proven. In fact, the convergence is uniform on compact sets. \square

The computation of $\text{res}(\lambda)$ reduces to a generalized eigenvalue problem. Let

$$U (= U(\lambda)) = J - \bar{\lambda} A - \lambda A^* + |\lambda|^2 G. \quad (3.40)$$

Then computing $\text{res}(\lambda)^2$ is equivalent to solving the minimization problem

$$\min_{c \in \mathbb{C}^N} c^* U c \quad \text{such that} \quad c^* G c = 1. \quad (3.41)$$

Let ξ be a Lagrange multiplier, that is, a necessary condition for s solution of 3.41 is

$$Uc - \xi Gc = 0 \quad (3.42)$$

since U and G are symmetric. Inserting such a c into the objective yields

$$c^* U c = c^* \xi G c = \xi \quad (3.43)$$

since $c^* G c = 1$. Hence 3.41 is solved by computing the smallest generalized eigenvalue solution of 3.42 (symmetry of U and G guarantees that all such eigenvalues are real).

Algorithm 2 Verification of candidate eigenpairs for \mathcal{K}

Require: Dictionary $\{\psi_j\}_{j=1}^N$, data points and weights $\{(w_i, x_i)\}_{i=1}^M$, tolerance ϵ

- 1: Perform algorithm 1 to obtain $G, A, KV = V\Lambda$
 - 2: Construct J as in 3.30
 - 3: **for** each candidate eigenpair (λ, v) **do**
 - 4: | Compute $\text{res}_{N,M}(\lambda, v)$ as in 3.41
 - 5: | Throw out λ if $\text{res}_{N,M}(\lambda, v) \geq \epsilon$
 - 6: **return** Verified Koopman (approximate-point) eigenvalues $\Lambda_M(\epsilon) = \{(\lambda, v) \mid \text{res}_{N,M}(\lambda, v) < \epsilon\}$
-

Algorithm 3 Residual EDMD to Compute $\sigma_{ap,\epsilon}(\mathcal{K})$

Require: Dictionary $\{\psi_j\}_{j=1}^N$, data points and weights $\{(w_i, x_i)\}_{i=1}^M$, grid $\{z_\nu\}_{\nu=1}^T \subset \mathbb{C}$, tolerance ϵ

- 1: Perform algorithm 1 to obtain G, A, K
 - 2: Construct J as in 3.30
 - 3: **for** z_ν **do**
 - 4: | Compute $\text{res}(z_\nu)$ as in 3.41
 - 5: **return** $\{z_\nu \mid \text{res}(z_\nu) < \epsilon\}$ as an approximation for $\sigma_{ap,\epsilon}(\mathcal{K})$
-

3.3.2 A Naive Attempt at Duality

From this point onward, we shall always assume (without loss of generality) that Ψ_X has full rank, that is, rank N when $N \leq M$ or rank M when $M \leq N$.

Algorithm 3 provides a way to compute the approximate-point pseudospectrum of the Koopman operator. In order to resolve the full pseudospectrum, one needs to compute $\sigma_{\inf}(\mathcal{K} - \lambda I)$ and $\sigma_{\inf}(\mathcal{L} - \bar{\lambda} I)$ for λ 's of interest. One could hope to perform the calculations in 3.34 backwards using \mathcal{L} instead of \mathcal{K} , but quickly notices that the inner product $\langle \mathcal{L}g, \mathcal{L}g \rangle$ or $g = \Psi c$ is not computable using just the information at hand.

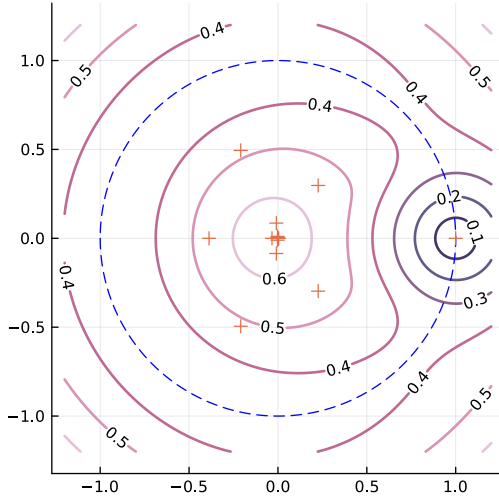


Figure 3.2: Algorithm 3 applied to the quadratic map (c.f. figure 2.1) performed with the same parameters as figure 3.1. Contours of $\lambda \mapsto \text{res}(\lambda)$ are shown with the spectrum of K . The quadratic map is ergodic [26] which is verified by the residuals. The eigenvalues of K other than 1 are spurious.

We instead try to follow the calculations forward. Starting with $L = G^{-1}A^*$ and $g = \Psi c$ we see that the analogous regression error for a candidate eigenpair can be written as

$$\|(\Psi_Y^* W \Psi_X - \lambda \Psi_X^* W \Psi_X) c\|_{\mathbb{C}^N}^2 = \|(\Psi_Y^* W - \lambda \Psi_X^* W) \Psi_X c\|_{\mathbb{C}^N}^2. \quad (3.44)$$

Notice that $\Psi_X^* W$ is precisely a quadrature approximation of Ψ^* from equation 3.19. $\Psi_X^* W$ takes an interpolation vector $f \in \mathbb{C}^M$ and approximates the integral with an interpolant function. Analogously we can deduce that $\Psi_Y^* W$ is a quadrature approximation of $(\mathcal{K}\Psi)^*$.

Assuming that $\{\psi_j\}_{j=1}^N$ is an orthonormal family, taking the infinite data limit

yields

$$\begin{aligned}
& \lim_{M \rightarrow \infty} \|(\Psi_Y^* W - \lambda \Psi_X^* W) \Psi_X c\|_{\mathbb{C}^N}^2 \\
&= \|((\mathcal{K}\Psi)^* - \lambda \Psi^*) g\|_{\mathbb{C}^N}^2 \\
&= \left\| \begin{pmatrix} \langle (\mathcal{K} - \lambda I)\psi_1, g \rangle \\ \vdots \\ \langle (\mathcal{K} - \lambda I)\psi_N, g \rangle \end{pmatrix} \right\|_{\mathbb{C}^N}^2 \\
&= \sum_{j=1}^N |\langle (\mathcal{K} - \lambda I)\psi_j, g \rangle|^2 \\
&= \sum_{j=1}^N |\langle \psi_j, (\mathcal{L} - \bar{\lambda}I)g \rangle|^2 \\
&= \|(\Pi \mathcal{L} \Pi - \bar{\lambda}I)g\|_{\mathcal{X}}^2
\end{aligned} \tag{3.45}$$

where P is the orthogonal projector onto $\text{span}\{\psi_j\}_{j=1}^N$. By the Galerkin property we know that L encodes precisely the action of $\Pi \mathcal{L} \Pi$. Hence,

$$\|(\Pi \mathcal{L} \Pi - \bar{\lambda}I)g\|_{\mathcal{X}}^2 = \|(L - \bar{\lambda}I)c\|_{\mathbb{C}^N}^2 \tag{3.46}$$

and so the least-squares Ansatz computes the pseudospectrum of L which by theorem 2.28 cannot be used analogously to algorithm 3 to compute $\sigma_{ap,\epsilon}(\mathcal{L})$. We would need to send $N \rightarrow \infty$ first, which would cause the equation $L = G^{-1}A^*$ to break.

While we will not use this immediately, we still expand the first line of 3.45 since we will see it again later.

$$\begin{aligned}
& \|(\Psi_Y^* W - \lambda \Psi_X^* W) \Psi_X c\|_{\mathbb{C}^N}^2 \\
&= \left\| \left(\Psi_Y^* \sqrt{W} - \lambda \Psi_X^* \sqrt{W} \right) \sqrt{W} \Psi_X c \right\|_{\mathbb{C}^N}^2 \\
&= \left(\sqrt{W} \Psi_X c \right)^* \sqrt{W} \left(\Psi_Y \Psi_Y^* - \bar{\lambda} \Psi_X \Psi_Y^* - \lambda \Psi_Y \Psi_X^* \right. \\
&\quad \left. + |\lambda|^2 \Psi_X \Psi_X^* \right) \sqrt{W} \left(\sqrt{W} \Psi_X c \right)
\end{aligned} \tag{3.47}$$

3.4 kernel EDMD (kEDMD)

3.4.1 The Kernel Trick

The choice of dictionary $\{\psi_j\}_{j=1}^N$ naturally has massive impacts on the accuracy of the above methods. We will see later in section 4 that a poorly chosen dictionary can cause catastrophic results. This is because even though there may be many ways to (in the limit $N \rightarrow \infty$) form a basis of \mathcal{X} , any practical

calculation will necessarily have a finite cut-off. So the challenge becomes finding efficient ways to increase N without needing to perform $O(N^2)$ quadrature problems.

One method which is enormously popular in machine learning [1, 6, 15, 22] is the so-called *kernel trick*. Consider the function $k : \mathbb{C}^2 \times \mathbb{C}^2 \rightarrow \mathbb{C}$, $(w, z) \mapsto (1 + w^*z)^2$. We can write this as

$$\begin{aligned} k(w, z) &= (1 + \bar{w}_1 z_1 + \bar{w}_2 z_2)^2 \\ &= (1 + 2\bar{w}_1 z_1 + 2\bar{w}_2 z_2 + 2\bar{w}_1 \bar{w}_2 z_1 z_2 + \bar{w}_1^2 z_1^2 + \bar{w}_2^2 z_2^2) \\ &= \langle \Psi(z), \Psi(w) \rangle_{\mathbb{C}^6} \quad (= \Psi(z)\Psi(w)^*) \end{aligned} \quad (3.48)$$

for the basis

$$\Psi(x) = [1 \mid \sqrt{2}x_1 \mid \sqrt{2}x_2 \mid \sqrt{2}x_1 x_2 \mid x_1^2 \mid x_2^2]. \quad (3.49)$$

While the result is the same, computation of $(1 + w^*z)^2$ requires only 5 floating-point operations, whereas $\Psi(z)\Psi(w)^*$ requires 23. More generally, any such relation $k(w, z) = \Psi(z)\Psi(w)^*$ is called a kernel trick.

Definition 3.7. A function $\Psi : \Omega \rightarrow \mathcal{Y}$ with $k(w, z) = \langle \Psi(z), \Psi(w) \rangle_{\mathcal{Y}}$ is known in machine learning literature as a feature map.

One sees that when $k(x, \cdot)$ is an element of some Hilbert space \mathcal{Y} , then an obvious kernel is given by $\Psi(x) = k(x, \cdot)$.⁶ Another obvious kernel is given by a basis: letting $\Psi(x) = [\psi_1(x) \mid \dots \mid \psi_N(x)]$ as before, $k(w, z) = \Psi(z)\Psi(w)^*$ is also a kernel.

Entire books are written on such kernels [24] and their properties. Common kernels include:

Example 3.8. The polynomial kernel $k : \mathbb{C}^d \times \mathbb{C}^d \rightarrow \mathbb{C}$, $(w, z) \mapsto (1 + w^*z/c^2)^\alpha$ feature map is given by all (multivariate) polynomials up to degree α . Note that computing $k(w, z)$ requires only $O(d)$ operations, but computing $\Psi(z)\Psi(w)^*$ requires superexponentially (in α) many combinations.

Example 3.9. The Gaussian kernel $k(w, z) = \exp\left(-\frac{\|w-z\|^2}{c^2}\right)$ has a feature map which is infinite-dimensional. Indeed, consider (for notational simplicity) $w, z \in \mathbb{R}$:

$$\begin{aligned} k(w, z) &= \exp\left(-\frac{|w|^2}{c^2}\right) \cdot \exp\left(\frac{2w \cdot z}{c^2}\right) \cdot \exp\left(-\frac{|z|^2}{c^2}\right) \\ &= \exp\left(-\frac{|w|^2}{c^2}\right) \cdot \left(\sum_{k=0}^{\infty} \frac{1}{k!} \left(\frac{2}{c^2}\right)^k (w \cdot z)^k\right) \cdot \exp\left(-\frac{|z|^2}{c^2}\right) \end{aligned} \quad (3.50)$$

⁶In fact, when Ψ also satisfies the *reproducing property*, that $\langle \Psi(x), f \rangle = f(x)$ for all $f \in \mathcal{Y}$, then \mathcal{Y} is known as *Reproducing Kernel Hilbert Space* and indeed $\text{span}\{k(x, \cdot) \mid x \in \Omega\}$ becomes dense in \mathcal{Y} .

so that

$$\Psi(x) = \exp\left(-\frac{|x|^2}{c^2}\right) \begin{bmatrix} 1 & \frac{\sqrt{2}}{c}x & \frac{1}{\sqrt{2!}}\left(\frac{\sqrt{2}}{c}x\right)^2 & \dots \end{bmatrix}. \quad (3.51)$$

When $w, z \in \mathbb{C}$ then the middle term in 3.50 changes from $w \cdot z$ to $\bar{w} \cdot z + \bar{z} \cdot w$, and in higher dimensions this extends to all pairwise combinations of the components of w and z . We note (and will use later) that in the specific case $\mathcal{X} = L^2(\mathbb{T})$ where \mathbb{T} is the (complex) unit circle, Ψ generates an orthogonal basis of \mathcal{X} , namely the Fourier basis.

3.4.2 Application to EDMD

Let k be a kernel with associated feature map Ψ that is rescaled such that

$$\Psi(x_j)\Psi(x_i)^* = \frac{k(x_i, x_j)}{\sqrt{w_i w_j}} \quad \text{for all } 1 \leq i, j \leq M. \quad (3.52)$$

In most cases $w_i = 1/M$ for all i so that the kernel is just scaled by a constant factor $1/M$.

Notice that

$$G = \Psi_X^* W \Psi_X = \sum_{i=1}^M w_i \Psi(x_i)^* \Psi(x_i), \quad A = \Psi_X^* W \Psi_Y = \sum_{i=1}^M w_i \Psi(x_i)^* \Psi(S(x_i)). \quad (3.53)$$

Each summand is a rank one matrix. This is not in a form where one could use the kernel trick, since we have summands of the form $\Psi(x_i)^* \Psi(x_i)$ instead of $\Psi(x_i) \Psi(x_i)^*$. However, if we reverse the order of multiplication in $\Psi_X^* W \Psi_X = (\sqrt{W} \Psi_X)^* (\sqrt{W} \Psi_X)$ then

$$\hat{G} = \sqrt{W} \Psi_X \Psi_X^* \sqrt{W} = (\sqrt{w_j w_i} \Psi(x_j) \Psi(x_i)^*)_{i,j=1}^M = (k(x_i, x_j))_{i,j=1}^M. \quad (3.54)$$

Analogously

$$\hat{A} = \sqrt{W} \Psi_Y \Psi_X^* \sqrt{W} = (k(S(x_i), x_j))_{i,j=1}^M. \quad (3.55)$$

We would now like to exploit the form of $K = \Psi_X^\dagger \Psi_Y$ to use these "flipped" matrices. The key to do so will be a (compact) singular value decomposition

$$\sqrt{W} \Psi_X = Q \Sigma Z^* \quad (3.56)$$

where $r = \min\{M, N\}$, $\Sigma \in \mathbb{R}_{\geq 0}^{r \times r}$ is a nonnegative diagonal matrix, and $Q \in \mathbb{C}^{M \times r}$ and $Z \in \mathbb{C}^{N \times r}$ are semi-unitary⁷.

⁷A tall matrix $M \in \mathbb{C}^{q \times r}$, $q \geq r$, is semi-unitary if the columns form an orthonormal family.

Theorem 3.10 ([31]). *Let*

$$\hat{K} := (\Sigma^\dagger Q^*) \hat{A} (Q\Sigma^\dagger). \quad (3.57)$$

Then (λ, c) (for $\lambda \neq 0$) is an eigenpair of \hat{K} iff (λ, Zc) is an eigenpair of K . Moreover, the eigenmodes $g = \Psi \cdot (Zc)$ can be evaluated at the data points x_i , $i = 1, \dots, M$.

One should take a moment to consider that the second statement made in the theorem seems highly nontrivial. Often, the feature map is only given implicitly - one knows there exists such a Ψ , but does not have an explicit form. Even worse, the matrix Z is completely unattainable from just \hat{G} and \hat{A} .

The benefit of using \hat{K} is that it can be computed in $O(M^2)$ time, *independent of N* . All that is required is an eigendecomposition for \hat{G} since by definition

$$\hat{G} = Q\Sigma^2Q^*. \quad (3.58)$$

Proof. Notice

$$Z\hat{K}Z^* = \Psi_X^\dagger \sqrt{W}^{-1} \sqrt{W} \Psi_Y \Psi_X^* \sqrt{W} \sqrt{W}^{-1} \Psi_X^* \dagger = K \Pi_{\text{ran } \Psi_X^* \sqrt{W}} \quad (3.59)$$

where $\Pi_{\text{ran } \Psi_X^*}$ is the orthogonal projection onto the range of Ψ_X^* . But since $\Psi_X^* \sqrt{W} = Z\Sigma Q^*$, this is equivalent to

$$\hat{K} = Z^* K Z \quad (3.60)$$

which immediately proves the first claim of the theorem. Now to evaluate $g = \Psi \cdot (Zc)$ at each x_i , $i = 1, \dots, M$, observe that $\Psi_X \cdot (Zc) = Q\Sigma c$. \square

Algorithm 4 Kernel EDMD

Require: kernel $k : \Omega \times \Omega \rightarrow \mathbb{C}$, data points and weights $\{(w_i, x_i)\}_{i=1}^M$, compression factor $r \leq M$

- 1: Construct \hat{G} , \hat{A} as in 3.54, 3.55
 - 2: Compute an eigendecomposition $\hat{G} = Q\Sigma^2Q^*$
 - 3: Let $\hat{\Sigma} = \Sigma[1:r, 1:r]$, $\hat{Q} = Q[:, 1:r]$ be the r largest eigenvalues and corresponding eigenvectors
 - 4: Construct $\hat{K} = (\hat{\Sigma}^\dagger \hat{Q}^*) \hat{A} (\hat{Q} \hat{\Sigma}^\dagger)$
 - 5: Compute an eigendecomposition $\hat{K}V = V\Lambda$
 - 6: **return** Eigenvalues and eigenvectors Λ, V
-

3.5 kernel ResDMD (kResDMD)

3.5.1 Associating a Residual to \hat{K}

We set out again to deduce which candidate eigenvalues produced by algorithm 4 are spurious, and which are accurate. Theorem 3.10 suggests that we could potentially compute $\|(\mathcal{K} - \lambda I)g\|$ by using the altered features $g = \Psi \cdot (Zv)$ the same way as in theorem 3.2. However, this is not effective in the regime $M \leq N$ (remember that the benefit of kernel methods was the ability to cheaply crank N up).

Proposition 3.11 ([10]). *Suppose $M \leq N$ and $\sqrt{W}\Psi_X \in \mathbb{C}^{M \times N}$ has full rank. Then for any eigenpair (λ, v) of \hat{K} , the residual*

$$\text{res}_{N,M}(\lambda, Zv) = 0. \quad (3.61)$$

Proof. Write

$$\sqrt{W}(\Psi_Y - \lambda\Psi_X)(Zv) = \sqrt{W}\Psi_Y Zc - \lambda Q\Sigma v = \sqrt{W}\Psi_Y \Psi_X^* \sqrt{W}Q\Sigma^\dagger c - \lambda Q\Sigma v. \quad (3.62)$$

Since $\sqrt{W}\Psi_X$ has full rank, the singular value matrix Σ in $\sqrt{W}\Psi_X = Q\Sigma Z^*$ is invertible, and so $\sqrt{W}\Psi_Y \Psi_X^* \sqrt{W}Q\Sigma^\dagger = Q\Sigma \hat{K}$. Inserting, we see

$$\sqrt{W}(\Psi_Y - \lambda\Psi_X)(Zv) = Q\Sigma(\hat{K} - \lambda I)v = 0. \quad (3.63)$$

□

The proposition suggests that we are suffering from *overfitting* of the snapshot data. We therefore require a different way to associate a residual to the eigenpair.

Recall from equation 3.28 that $\text{res}_{N,M}$ has an alternative representation as a regression error. We could analogously ask if \hat{K} is the solution of a different regression problem.

Let

$$\widehat{\Psi}_X = \left(\sqrt{W}\Psi_X \right)^* Q\Sigma^\dagger = Z, \quad \widehat{\Psi}_Y = \left(\sqrt{W}\Psi_Y \right)^* Q\Sigma^\dagger. \quad (3.64)$$

Then we have

$$\widehat{\Psi}_X^\dagger \widehat{\Psi}_Y = Z^* \left(\sqrt{W}\Psi_Y \right)^* Q\Sigma^\dagger = (\Sigma^\dagger Q^*) \left(\sqrt{W}\Psi_X \Psi_Y^* \sqrt{W} \right) (Q\Sigma^\dagger) = \hat{K}^*. \quad (3.65)$$

Hence \hat{K}^* is precisely the solution to the least squares problem

$$\min_{B \in \mathbb{C}^{M \times M}} \left\| \widehat{\Psi}_Y - \widehat{\Psi}_X B \right\|. \quad (3.66)$$

This means that for a candidate eigenpair (λ, c) of \hat{K}^* , the regression error is given by

$$\widehat{\text{res}}_{N,M}(\lambda, v) = \left\| \left(\widehat{\Psi}_Y - \lambda \widehat{\Psi}_X \right) v \right\|. \quad (3.67)$$

To provide a computable formulation we write

$$\widehat{\text{res}}_{N,M}(\lambda, v)^2 = \left\| (\Psi_Y^* - \lambda \Psi_X^*) \sqrt{W} (Q \Sigma^\dagger c) \right\|^2 \quad (3.68)$$

which, after expanding the squared norm as in equation 3.33, can be written as

$$v^* (\Sigma^\dagger Q^*) \left(\sqrt{W} \Psi_Y \Psi_Y^* \sqrt{W} - \bar{\lambda} \widehat{A} - \bar{\lambda} \widehat{A}^* + |\lambda|^2 \widehat{G} \right) (Q \Sigma^\dagger) v. \quad (3.69)$$

Notice $(\Sigma^\dagger Q^*) \widehat{G} (Q \Sigma^\dagger) = I$ and $(\Sigma^\dagger Q^*) \widehat{A} (Q \Sigma^\dagger) = \widehat{K}$. Finally, letting

$$\widehat{J} = \sqrt{W} \Psi_Y \Psi_Y^* \sqrt{W} = (k(S(x_i), S(x_j)))_{i,j=1}^M \quad (3.70)$$

we have that

$$\widehat{\text{res}}_{N,M}(\lambda, v)^2 = v^* \left((\Sigma^\dagger Q^*) \widehat{J} (Q \Sigma^\dagger) - \bar{\lambda} \widehat{K} - \lambda \widehat{K}^* + |\lambda|^2 I \right) v. \quad (3.71)$$

At this point it is unclear whether $\widehat{\text{res}}$ has any physical meaning. It is an error metric for some arbitrary seeming least squares regression problem with matrices $\widehat{\Psi}_X$ and $\widehat{\Psi}_Y$ which do not have a clear interpretation. The current state of research in this kernelized method stops here.

However, the fact that the *adjoint* \widehat{K}^* solves the least squares problem, should give the reader a suspicion that the least squares problem might have more to do with the Perron-Frobenius operator than with the Koopman operator.

Algorithm 5 Kernel ResDMD

Require: kernel $k : \Omega \times \Omega \rightarrow \mathbb{C}$, data points and weights $\{(w_i, x_i)\}_{i=1}^M$, compression factor $r \leq M$, grid $\{z_\nu\}_{\nu=1}^T \subset \mathbb{C}$, tolerance ϵ

- 1: Construct \widehat{G} , \widehat{A} as in 3.54, 3.55
 - 2: Compute an eigendecomposition $\widehat{G} = Q \Sigma^2 Q^*$
 - 3: Let $\widehat{\Sigma}$, \widehat{Q} be as in algorithm 4
 - 4: Construct \widehat{K} , \widehat{J} as in 3.57, 3.70 (with \widehat{Q} and $\widehat{\Sigma}$)
 - 5: **for** z_ν **do**
 - 6: **Compute** $\widehat{\text{res}}(z_\nu) := \min_{\|v\|=1} \widehat{\text{res}}(z_\nu, v)$, which is equivalent to finding the smallest eigenvalue of the matrix in 3.71
 - 7: **return** $\{z_\nu \mid \widehat{\text{res}}(z_\nu) < \epsilon\}$
-

3.5.2 The Perron-Frobenius Connection

It is worth reexamining equation 3.60. Returning for a moment to the case $N \leq M$ we have

$$\begin{aligned}\widehat{K}^* &= Z^* K^* Z \\ &= Z^* A^* G^{-1} Z \\ &= Z^* G G^{-1} A^* G^{-1} Z \\ &= (Z^* G) L(G^{-1} Z) \\ &= (\Sigma^2 Z^*) L(\Sigma^2 Z^*)^\dagger\end{aligned}\tag{3.72}$$

where we used that G is symmetric and (when $N \leq M$) invertible. While this may not be true in $N \geq M$, there still is one connection: compare equations 3.47 and 3.69. One sees that up to conjugation of λ and multiplication of a factor $\Sigma^2 Z^*$ they coincide exactly.

Since Q and Z are both finite-dimensional isometries, they do not affect the minimal value of 3.47 or 3.69. In the regime $N \leq M$, $G = Z\Sigma^2 Z^*$, Σ^2 holds the norm of the features after being linearly combined into an \mathcal{X} -orthogonal basis. Hence $Q\Sigma^\dagger$ in

$$\widehat{\text{res}}_{N,M}(\lambda)^2 = \min_{\|v\|=1} v^* (\Sigma^\dagger Q^*) \left(\widehat{J} - \bar{\lambda} \widehat{A} - \lambda \widehat{A}^* + |\lambda|^2 \widehat{G} \right) (Q\Sigma^\dagger) v \tag{3.73}$$

serves the same purpose as the stiffness matrix G in

$$\widetilde{\text{res}}_{N,M}(\lambda)^2 := \min_{c^* G c = 1} (\Psi_X c)^* \left(\widehat{J} - \lambda \widehat{A} - \bar{\lambda} \widehat{A}^* + |\lambda|^2 \widehat{G} \right) (\Psi_X c). \tag{3.74}$$

In particular we see that there must exist C_1, C_2 such that

$$C_1 \cdot \widehat{\text{res}}_{N,M}(\lambda) \leq \widetilde{\text{res}}_{N,M}(\bar{\lambda}) \leq C_2 \cdot \widehat{\text{res}}_{N,M}(\lambda) \tag{3.75}$$

so that algorithm 5 computes precisely the (scaled) pseudospectrum of $\Pi \mathcal{L} \Pi$ as in 3.46.

So what happens in the regime $N \geq M$? In this regime, $L = G^{-1} A^*$ breaks down since $\Psi_X^\dagger = (\Psi_X^* \Psi_X)^{-1} \Psi_X^*$ no longer holds (rather, $\Psi_X^\dagger = \Psi_X^* (\Psi_X \Psi_X^*)^{-1}$). Nonetheless, $\widehat{\text{res}}$ is still well-defined, it just loses its physical meaning.

4 Benchmark Examples

Having studied the current most popular Koopman operator approximation scheme in theory, it is time to set it in practice. Figures 2.1, 2.2, 3.1, 3.2 already show convincing results. We continue with three more results, showing both advantages and disadvantages of dynamic mode decompositions.

4.1 Duffing Oscillator

We apply algorithm 3 on the unforced duffing equation [13]

$$\ddot{x} = -\delta\dot{x} - x(\beta + \alpha x^2) \quad (4.1)$$

using the parameters $\alpha = 1$, $\beta = -1$, $\delta = 1/2$ as in [30]. Viewing this as a two-dimensional first order ODE in the coordinates x and \dot{x} , the system has two basins of attraction, see figure 4.1. We use a cartesian grid quadrature scheme consisting 500 Gauß-Legendre nodes and weights in each dimension (transplanted onto the domain $[-2, 2]$), resulting in a total of $M = 2500$ nodes. For a dictionary we use products of Legendre polynomials

$$(x, \dot{x}) \mapsto P_k(x/2) \cdot P_l(\dot{x}/2) \quad (4.2)$$

for $k, l = 0, \dots, 9$, totalling $N = 100$ dictionary functions. We approximate the continuous-time ODE system by time-stepping with step size $\Delta t = 0.1$. The first 3 nontrivial eigenfunctions of K are shown in figure 4.2.

The two stable equilibria located at $x = \pm\sqrt{\frac{\beta}{\alpha}}$, $\dot{x} = 0$ are *eigendistributions* in the sense that Dirac deltas centered at the equilibria are invariant under \mathcal{K} . EDMD attempts to resolve these Dirac distributions using the available basis, resulting in two fast growing functions with support localized as much as possible on the equilibria. Also visible are the two basins of attraction approximated by the sign of the second largest eigenvalue.

Finally, an almost-invariant set is seen tracing the boundary of the two basins. Indeed, the basin of attraction for the unstable equilibrium at the origin is precisely the two trajectories tracing the boundaries of the basins for the other equilibria. This infinitesimal basin is approximated by smooth functions, resulting in an artificial widening of the numerically computed basin. Not visible is the Dirac eigendistribution at the unstable equilibrium. This is because there was not a data point centered at this equilibrium, and its instability caused points to be mapped away too quickly.

4.2 Alanine Dipeptide

Alanine dipeptide is a biomolecule which is used as a standard nontrivial test case for macroscopic dynamics [16]. Typical energy-optimization based methods to determine stable conformations are difficult to use due to many local minima existing [21]. It is shown in [21] that the shape (and therefore chemical reaction properties) are determined primarily by only two *dihedral angles* in the backbone of the molecule (see figure 4.3).

We use trajectory data of the heavy atoms gathered from experiments in [23]. After subsampling the trajectory data to use just every 50th time steps, we obtain $M = 2500$ data points in \mathbb{R}^{30} . We apply algorithm 5 using the Gaußian

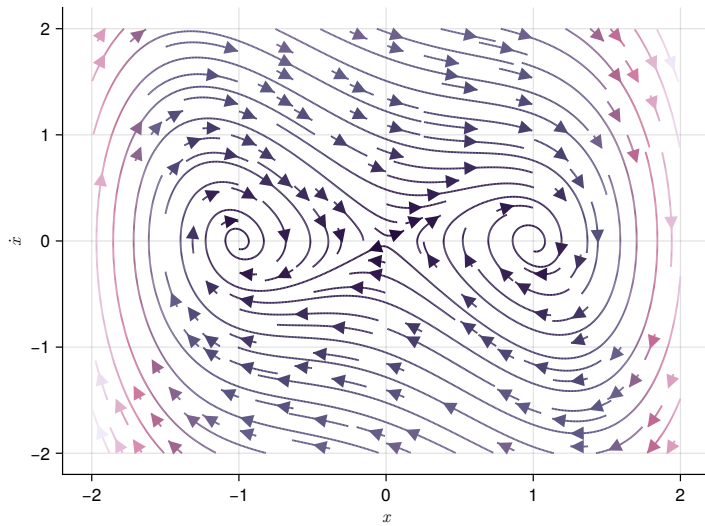


Figure 4.1: Phase portrait of the Duffing equation 4.1.

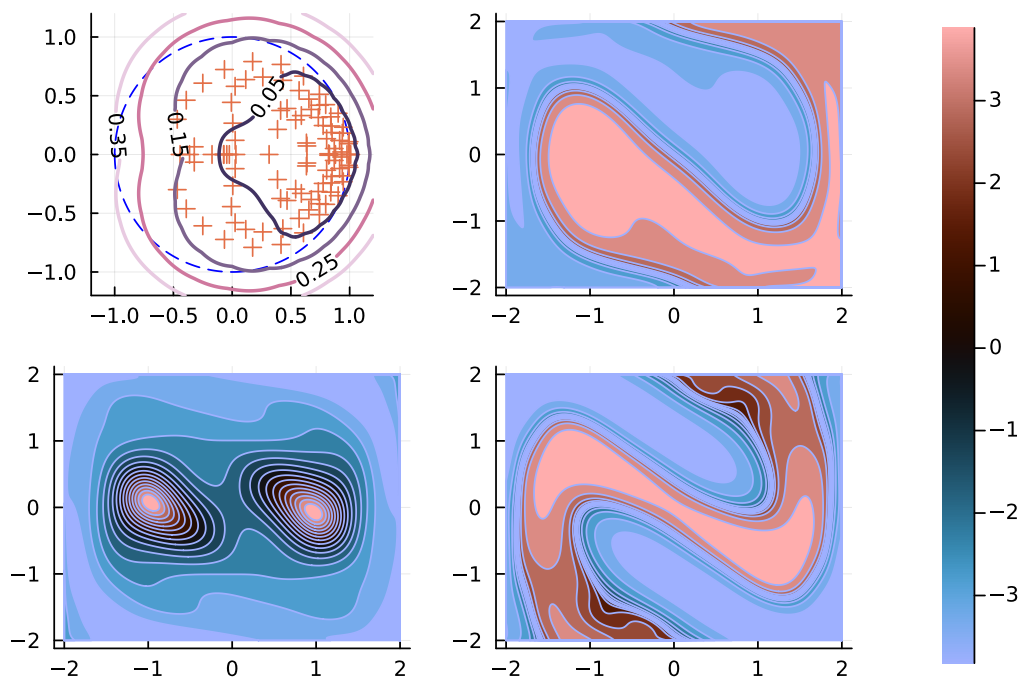


Figure 4.2: Spectrum of the Duffing equation. Top left: Spectrum of K (orange) with residuals computed from algorithm 3. The other plots are the real parts of the first 3 nontrivial eigenfunctions for K . See section 4.1 for analysis.

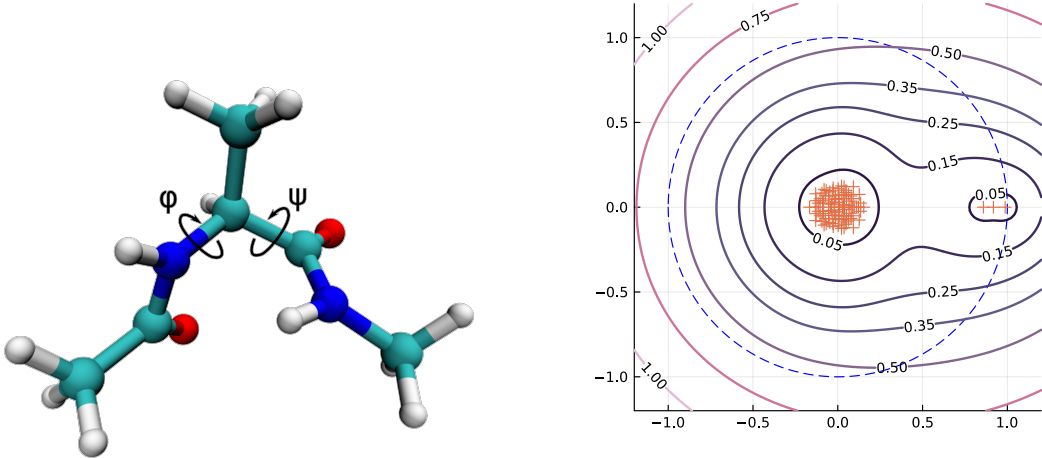


Figure 4.3: Left: alanine dipeptide molecule skeleton. The *dihedral angles* φ and ψ are the primary determining factors of the shape and chemical reaction properties of the molecule. Right: spectrum of \widehat{K} with residuals computed from algorithm 5. See section 4.2 for analysis.

kernel 3.50 with parameter $c^2 = 0.01$. The spectrum of \widehat{K} is shown in figure 4.3; figure 4.4 shows the two nontrivial eigenfunctions, projected into the space spanned by the two dihedral angles.

It is highly important to note that no a priori information was used to choose observables, determine the subsampling method, or tune the kernel parameter. The dihedral angles are used purely for plotting.

After obtaining the two nontrivial eigenfunctions, k -means clustering was used with $k = 3$ clusters, to determine the metastable sets in \mathbb{R}^{30} . The projection of these sets into the space spanned by the two dihedral angles is shown in figure 4.5. Indeed, these are the same metastable conformations as experimentally observed in [21].

4.3 Blaschke Products

4.3.1 Definition

As a final model we consider a family of (complex) analytic circle maps

$$S : \mathbb{T} \rightarrow \mathbb{T}, \quad z \mapsto z \frac{z - \mu}{1 - \bar{\mu}z} \quad (4.3)$$

for $\mu \in \mathbb{D}$ in the open unit disk. S is a two-to-one map on the circle which can be analytically extended to the annulus $A_\mu = \{z \in \mathbb{C} \mid |\mu| < |z| < |\mu|^{-1}\}$. The Perron-Frobenius operator spectrum has been studied analytically in [4]. It is shown (with much effort) that on a subspace of $L^2(\mathbb{T})$ containing certain

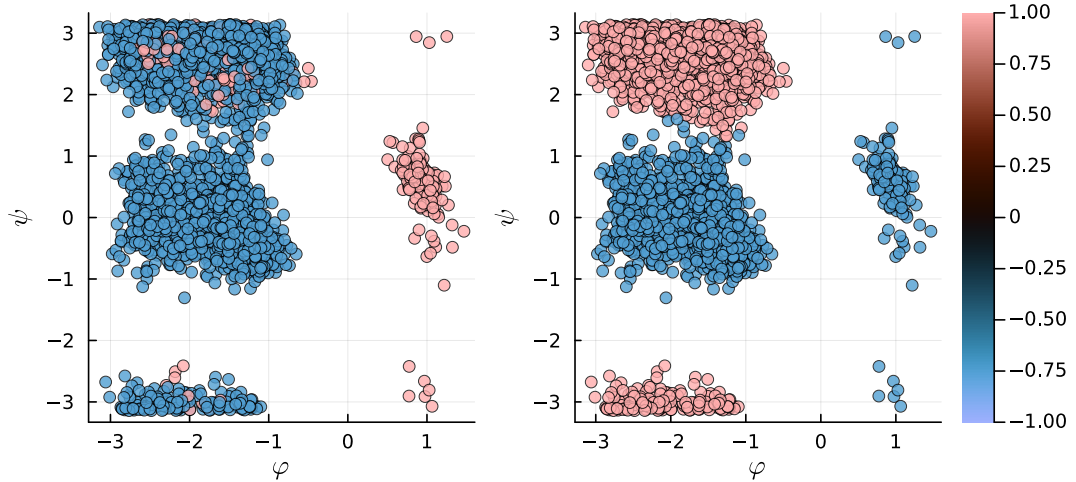


Figure 4.4: First two nontrivial eigenfunctions of \hat{K} for the alanine dipeptide molecule, projected into the space of the two dihedral angles. Note that \hat{K} is computed with the full 30-dimensional data and the observables use no a priori information on the dihedral angles.

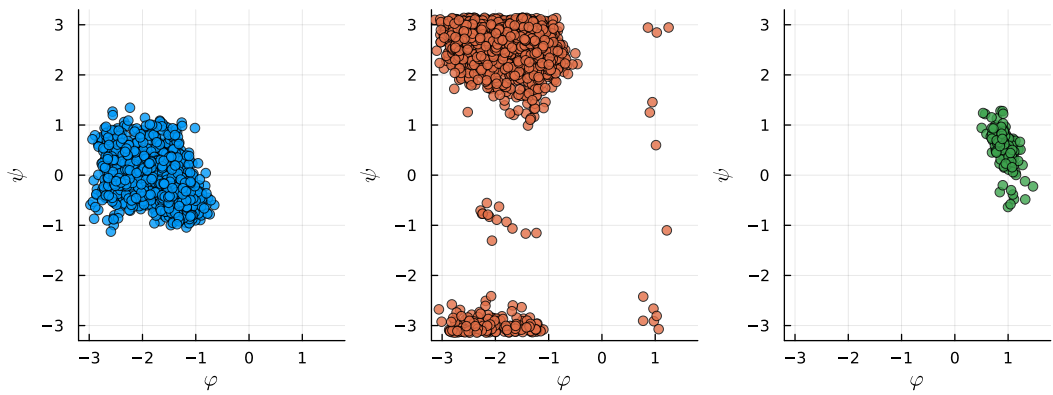


Figure 4.5: k-means clustering of the almost invariant sets, projected into the space of the two dihedral angles.

holomorphic functions, \mathcal{L} is compact and has a simple spectrum. More specifically, let $H(A_r)$ denote the set of holomorphic functions on an annulus A_r , $r < 1$, and $H^2(A_r)$ the subspace of holomorphic functions which are square integrable on the boundary $\partial A = \{z \in \mathbb{C} \mid |z| = r \text{ or } 1/r\}$.

This space (known as a Hardy space) is Hilbert with inner product

$$\langle f, g \rangle_{H^2(A_r)} = \left[\lim_{\rho \searrow r} \frac{1}{2\pi i} \int_{\partial B_\rho} \overline{f(z)} \cdot g(z) \frac{dz}{z} \right] + \left[\lim_{\rho \nearrow \frac{1}{r}} \frac{1}{2\pi i} \int_{\partial B_\rho} \overline{f(z)} \cdot g(z) \frac{dz}{z} \right]. \quad (4.4)$$

It is not hard from here to see that $e_n(z) = z^n / \sqrt{r^{2n} + r^{-2n}}$ is an orthonormal basis.

We do not make much use of the structure of $H^2(A)$ at first, aside from taking note that $H^2(A)$ is a strict subset of $L^2(\mathbb{T})$.

Proposition 4.1 ([4]). *Let S be a Blaschke product of the form 4.3 and A_r be a suitably chosen annulus⁸ containing \mathbb{T} . Then $\mathcal{L}|_{H^2(A)}$ is compact⁹ and*

$$\sigma(\mathcal{L}|_{H^2(A)}) = \sigma_p(\mathcal{L}|_{H^2(A)}) = \{\mu^n \mid n \in \mathbb{N}_0\} \cup \{\bar{\mu}^n \mid n \in \mathbb{N}_0\}. \quad (4.5)$$

As a consequence of $H^2(A) \subset L^2(\mathbb{T})$,

$$\{\mu^n \mid n \in \mathbb{N}_0\} \cup \{\bar{\mu}^n \mid n \in \mathbb{N}_0\} \subset \sigma_p(\mathcal{L}|_{L^2(\mathbb{T})}). \quad (4.6)$$

We note that, in its default form, algorithms 1, 4 attempt to compute $\sigma_p(\mathcal{K}|_{L^2(\mathbb{T})})$.

4.3.2 An Initial Numerical Experiment

With this context, we use algorithm 3 for the Blaschke product, with $\mu = \frac{3}{4}e^{i\pi/4}$. As a first attempt, we try again using Gauß-Legendre quadrature by reparameterizing the circle onto $[-1, 1]$. We use $M = 1000$ quadrature nodes and $N = 40$ Legendre polynomials as a dictionary. The numerically computed spectrum is shown in figure 4.6. Aside from the trivial (constant) invariant eigenfunction, the spectrum of L is entirely unrelated to the true spectrum.

However, when we perform the same experiment using the same number of quadrature nodes, this time equally spaced, and a *Fourier basis* $c_n(\theta) = e^{i\pi n \theta}$, $n = -20, \dots, 20$, then the spectrum of L matches the true spectrum exactly. In fact, in [2] it is shown that (when enough quadrature nodes are used) the approximated spectrum converges to the true spectrum *exponentially* in N .

⁸By the expansivity of S , we can choose annuli $A_0 \subset\subset A' \subset\subset A$ such that $S(\partial A_0) \cap \overline{A} = \emptyset$. These conditions are necessary for well-definedness of $\mathcal{L}|_{H^2(A)}$ [3]. Here, " $A' \subset\subset A$ " means that the closure of A' is a strict subset of A .

⁹In fact, $\mathcal{L}|_{H^2(A)}$ is Hilbert-Schmidt.

What remains unclear is why the residuals computed using algorithm 3 are still large in both the Legendre and Fourier experiments. If one were to rely on the residuals computed by algorithm 3, one would reject these eigenvalues as spurious. To understand this we recall theorem 2.9 and corollary 2.21. The problem lies in the *residual spectrum*. Indeed, the *point* spectrum of $\mathcal{K}|_{L^2(\mathbb{T})}$ does not include any of $\{\mu^n \mid n \in \mathbb{N}_0\} \cup \{\bar{\mu}^n \mid n \in \mathbb{N}_0\}$ aside from the trivial invariant eigenfunction.

However, since the Fourier basis is clearly orthonormal on $L^2(\mathbb{T})$, we have $G = I$ so that $L = K^*$. Additionally, finite-dimensional operators only have point spectrum and so $\sigma_p(K) = \sigma_p(L)$. Hence the seeming accuracy of $\sigma(K)$ is a reflection of the fact that $\sigma(L)$ approximates $\sigma(\mathcal{L}|_{H^2(A)})$ exponentially well.

Nonetheless, one still can use ResDMD to verify the eigenvalues which are computed, one just needs to do so over the "correct" space. Since for $n > 0$, $\mu^n \notin \sigma_p(\mathcal{K}|_{L^2(\mathbb{T})})$ but $\mu^n \in \sigma_p(\mathcal{L}|_{L^2(\mathbb{T})})$, we must have $\mu^n \in \sigma_r(\mathcal{K}|_{L^2(\mathbb{T})})$. From theorem 2.9, $\mu^n \in \sigma_p(\mathcal{K}|_{H^2(A)^*})$ where $H^2(A)^*$ is the Banach space adjoint of $H^2(A)$ embedded in $L^2(\mathbb{T})$. We therefore must investigate the structure of $H^2(A)^*$.

4.3.3 The Adjoint of $H^2(A)$

Let $\mathbb{D}_r = \{z \in \mathbb{C} \mid |z| < r\}$ and $H^2(\mathbb{D}_r^\infty)$ be the set of functions holomorphic on $\mathbb{C} \setminus \overline{\mathbb{D}_r}$ which are square integrable on the boundary $\partial\mathbb{D}_r$ and vanish at infinity, that is

$$H^2(\mathbb{D}_r) = \left\{ f \in H(\mathbb{D}_r) \mid \langle f, f \rangle_{H^2(\mathbb{D}_r)} = \lim_{\rho \nearrow r} \int_{\partial B_\rho} \overline{f(z)} f(z) \frac{dz}{z} < \infty \right\} \quad (4.7)$$

$$\begin{aligned} H^2(\mathbb{D}_r^\infty) &= \left\{ f \in H(\mathbb{C} \setminus \mathbb{D}_r) \mid \lim_{|z| \rightarrow \infty} f(z) = 0 \text{ and} \right. \\ &\quad \left. \langle f, f \rangle_{H^2(\mathbb{D}_r^\infty)} = \lim_{\rho \searrow r} \int_{\partial B_\rho} \overline{f(z)} f(z) \frac{dz}{z} < \infty \right\} \end{aligned} \quad (4.8)$$

Theorem 4.2 ([3]). *The Banach space adjoint of $H^2(A_r) \subset L^2(\mathbb{T})$ is isomorphic to the direct sum $H^2(\mathbb{D}_r) \oplus H^2(\mathbb{D}_{\frac{1}{r}}^\infty)$.*

Some elementary complex analysis shows that

$$H^2(\mathbb{D}_r) = \left\{ f = \sum_{n=0}^{\infty} c_n z^n \in H(\mathbb{D}_r) \mid \sum_{n=0}^{\infty} |c_n|^2 r^{2n} < \infty \right\} \quad (4.9)$$

and analogously

$$H^2(\mathbb{D}_{\frac{1}{r}}^\infty) = \left\{ f = \sum_{n=1}^{\infty} c_{-n} z^{-n} \in H(\mathbb{D}_r) \mid \sum_{n=1}^{\infty} |c_{-n}|^2 r^{2n} < \infty \right\}. \quad (4.10)$$

Hence the space $\mathcal{X} = H^2(\mathbb{D}_r) \oplus H^2(\mathbb{D}_{\frac{1}{r}}^\infty)$ can be characterized by the norm

$$\|f\|_{\mathcal{X}}^2 = \left\| \sum_{n=-\infty}^{\infty} c_n z^n \right\|_{\mathcal{X}}^2 = \sum_{n=-\infty}^{\infty} |c_n|^2 r^{2|n|}. \quad (4.11)$$

Notice that the coefficients c_n are precisely the Fourier coefficients of f . The triple $H^2(A) \subset L^2(\mathbb{T}) \subset H^2(A)^* = \mathcal{X}$ is known as a Gelfand triple or rigged Hilbert space. In particular the space \mathcal{X} is distributional, it is strictly larger than $L^2(\mathbb{T})$.

Knowing that

$$\sigma\left(\mathcal{L}|_{H^2(A)}\right) \setminus \{0\} = \sigma_p\left(\mathcal{L}|_{H^2(A)}\right) \setminus \{0\} \subset \sigma_r\left(\mathcal{K}|_{L^2(\mathbb{T})}\right) \quad (4.12)$$

and that

$$\sigma\left(\mathcal{L}|_{H^2(A)}\right) = \sigma\left(\mathcal{K}|_{H^2(A)^*}\right) \quad (4.13)$$

we can conclude

$$\sigma\left(\mathcal{K}|_{H^2(A)^*}\right) = \sigma_p\left(\mathcal{K}|_{H^2(A)^*}\right) = \{\mu^n \mid n \in \mathbb{N}_0\} \cup \{\bar{\mu}^n \mid n \in \mathbb{N}_0\}. \quad (4.14)$$

We have therefore arrived (in an alternative manner) at the main result of [3].

We may now use this knowledge to perform algorithm 3 in this space. Recall equations 3.13, 3.14, 3.30 suggest that we can approximate G by

$$G_{ij} \approx \langle \psi_i, \psi_j \rangle_{\mathcal{X}} = \sum_{n=-\infty}^{\infty} \overline{c_n(\psi_i)} c_n(\psi_j) r^{2|n|} \quad (4.15)$$

and analogous for A and J . The result of doing so with the same fourier basis as before results in figure 4.7. Indeed, both the eigenvalues and residuals verify the analytically deduced spectrum of $\mathcal{K}|_{H^2(A)^*}$.

It is worth taking a moment to consider what has happened, as it is quite unintuitive. When we *shrunk* the domain of \mathcal{L} , we removed all element of the spectrum which were not in the point spectrum. Correspondingly in the dual, we *enlarged* the domain until elements of the residual spectrum became elements of the point spectrum. By adding the necessary function(als) to the domain, we were able to find new elements of the kernel of $\mathcal{K} - \lambda I$. This is the *only* way that this can happen. An element of the residual spectrum can (by theorem 2.9) not convert into continuous spectrum.

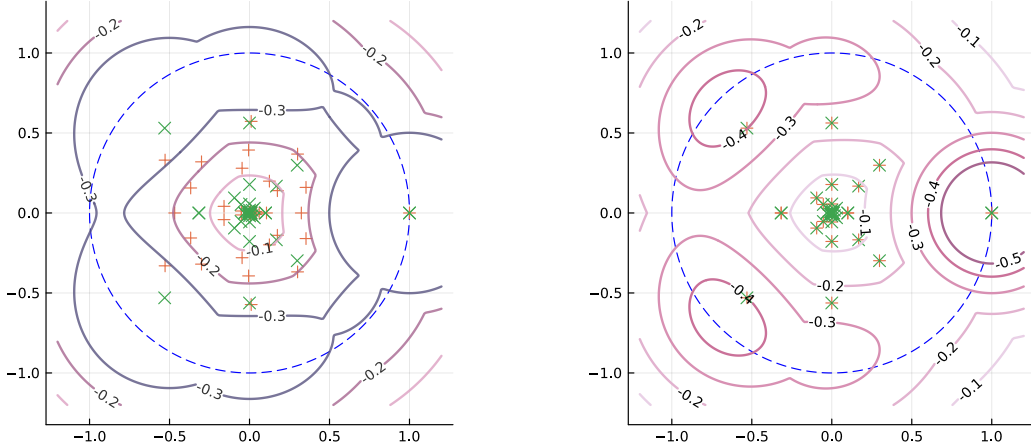


Figure 4.6: Left: spectrum of L with residuals calculated using algorithm 3, when using an approximation space consisting of 40 Legendre polynomials. Right: The same calculation using an approximation space of Fourier modes. In both cases, green: true spectrum of $\mathcal{L}|_{H^2(A)}$, orange: spectrum of the EDMD matrix L . See section 4.3.2 for analysis.

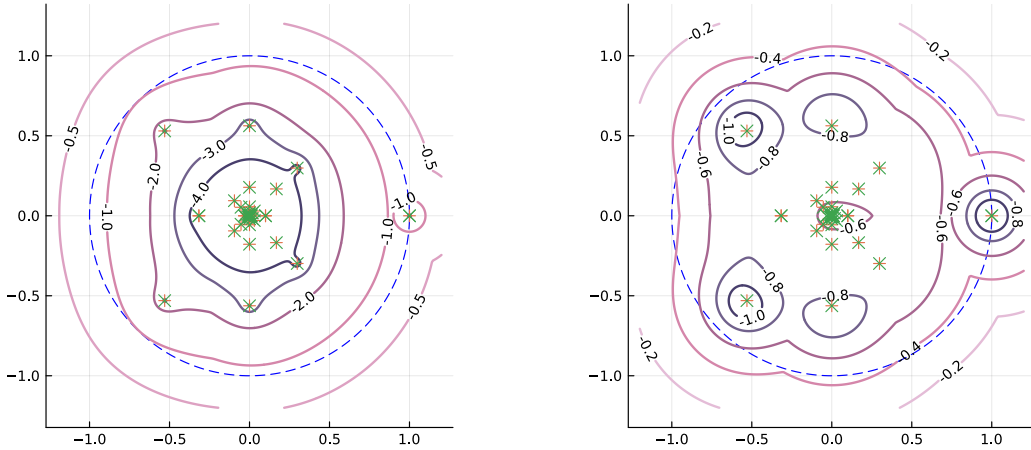


Figure 4.7: Left: spectrum of \hat{K} with residuals calculated using algorithm 5, logarithmically scaled. Contour lines show approximated ϵ -pseudospectrum for $\epsilon = 10^{-2}, 10^{-1}, 10^{-0.8}, 10^{-0.6}, 10^{-0.5}, 10^{-0.4}, 10^{-0.2}$. Right: residuals calculated using the inner product $\langle \cdot, \cdot \rangle_{H^2(A)^*}$. In both cases, green: true spectrum of $\mathcal{L}|_{H^2(A)}$, orange: spectrum of the approximated matrix (left \hat{K} , right K using the dual Hardy inner product). See section 4.3.3 for analysis.

5 Conclusion

5 related algorithms for the study of Koopman and Perron-Frobenius operators are studied. The algorithms are based on the concept of *pseudospectra*, which are investigated from a theoretical basis before applied to Koopman operators. In the process, two new proofs (one extension and one correction of previous proofs) are given for well-known results in pseudospectral theory. The idea behind each algorithm is deduced rigorously, and new connections between algorithms are presented. Finally, the algorithms are explored on three examples.

The examples lead to a fundamental question in the study of operator theoretic dynamics, which was already hinted toward in the example of the Duffing equation. When the physically relevant (pseudo)eigenvectors lie outside of the space of study, as e.g. Dirac distributions on equilibria and periodic orbits, or e.g. adjoint Hardy space functionals, how should one know which approximated eigenvectors are "real"?

This interesting phenomenon that many discretization techniques are excited by eigenmodes of Koopman operators over functions spaces which are *strictly larger* than L^2 . This raises a question - which computed eigenmodes are (1) "expected": approximations of L^2 Koopman eigenmodes, (2) "unexpected": approximations of eigenmodes in unintended function spaces, (3): "spurious": caused solely by the discretization?

The current state of research holds two potential answers to this question, the first of which has already been mentioned in section 3.3.1: one can make a philosophical change and assume that the underlying dynamics is governed by a stochastic system. The result of this assumption is that \mathcal{K} (resp. \mathcal{L}) "collapses" to a compact operator. In this case one can construct *strongly* convergent approximation schemes e.g. Ulams' method [12] or point-cloud methods based on entropically regularized optimal transport [16]. However, the stochastic approach "destroys fine structures" in the sense that anything which is not robust to perturbation is changed, e.g. fixed points become absolutely continuous invariant measures with (potentially) support on the entire phase space.

Another approach [9] considers only measure preserving dynamical systems (thereby restricting to the case that \mathcal{K} is an isometry) but tackles continuous and point spectrum simultaneously by embedding some space \mathcal{X} into a *rigged Hilbert space* structure, $\mathcal{X} \subset L^2(\Omega) \subset \mathcal{X}^*$. By carefully choosing this approximation space, one can guarantee a existence of a full spectral decomposition of \mathcal{K} .

More research into the regime $N < M$ may lead to further connections between kernel methods and Perron-Frobenius methods.

References

- [1] Mark A. Aizerman, E. M. Braverman, and Lev I. Rozonoer. “Theoretical foundation of potential functions method in pattern recognition”. In: 2019. URL: <https://api.semanticscholar.org/CorpusID:92987925>.
- [2] Elliz Akindji et al. *Convergence properties of dynamic mode decomposition for analytic interval maps*. 2024. arXiv: 2404.08512 [math.DS]. URL: <https://arxiv.org/abs/2404.08512>.
- [3] Oscar F. Bandtlow, Wolfram Just, and Julia Slipantschuk. *Spectral structure of transfer operators for expanding circle maps*. 2013. arXiv: 1311.3122 [math.DS]. URL: <https://arxiv.org/abs/1311.3122>.
- [4] Oscar F. Bandtlow, Wolfram Just, and Julia Slipantschuk. “Spectral structure of transfer operators for expanding circle maps”. In: *Annales de l’Institut Henri Poincaré C, Analyse non linéaire* 34.1 (2017), pp. 31–43. ISSN: 0294-1449. DOI: <https://doi.org/10.1016/j.anihpc.2015.08.004>.
- [5] A. Boettcher and S.M. Grudsky. *Spectral Properties of Banded Toeplitz Matrices*. Society for Industrial and Applied Mathematics, 2005. ISBN: 9780898717853.
- [6] Colin Campbell. “An introduction to kernel methods”. In: *Studies in Fuzziness and Soft Computing* 66 (2001), pp. 155–192.
- [7] F. Chaitin-chatelin. “About Definitions of Pseudospectra of Closed Operators in Banach Spaces”. In: (May 2000).
- [8] Matthew J. Colbrook. “Chapter 4 - The multiverse of dynamic mode decomposition algorithms”. In: *Numerical Analysis Meets Machine Learning*. Ed. by Siddhartha Mishra and Alex Townsend. Vol. 25. Handbook of Numerical Analysis. Elsevier, 2024, pp. 127–230. DOI: <https://doi.org/10.1016/bs.hna.2024.05.004>.
- [9] Matthew J. Colbrook, Catherine Drysdale, and Andrew Horning. *Rigged Dynamic Mode Decomposition: Data-Driven Generalized Eigenfunction Decompositions for Koopman Operators*. 2024. arXiv: 2405.00782 [math.DS]. URL: <https://arxiv.org/abs/2405.00782>.
- [10] Matthew J. Colbrook and Alex Townsend. “Rigorous data-driven computation of spectral properties of Koopman operators for dynamical systems”. In: *Communications on Pure and Applied Mathematics* 77.1 (2024), pp. 221–283. DOI: <https://doi.org/10.1002/cpa.22125>.
- [11] Jianlian Cui, Chi-Kwong Li, and Yiu-Tung Poon. “Pseudospectra of special operators and pseudospectrum preservers”. In: *Journal of Mathematical Analysis and Applications* 419.2 (2014), pp. 1261–1273. ISSN: 0022-247X. DOI: <https://doi.org/10.1016/j.jmaa.2014.05.041>.
- [12] Michael Dellnitz and Oliver Junge. “On the Approximation of Complicated Dynamical Behavior”. In: *SIAM Journal on Numerical Analysis* 2.36 (1999).

- [13] G. Duffing. *Erzwungene Schwingungen bei veränderlicher Eigenfrequenz und ihre technische Bedeutung*. Sammlung Vieweg. Vieweg, 1918. URL: <https://books.google.de/books?id=s3W4AAAAIAAJ>.
- [14] Paul Garrett. *Exmaples of Operators and Spectra*. Online. 2020. URL: http://www.math.umn.edu/%CB%9Cgarrett/m/fun/notes_2012-13/06b_examples_spectra.pdf.
- [15] Thomas Hofmann, Bernhard Schölkopf, and Alexander J Smola. “Kernel methods in machine learning”. In: (2008).
- [16] Oliver Junge, Daniel Matthes, and Bernhard Schmitzer. *Entropic transfer operators*. 2023. eprint: 2204.04901. URL: <https://arxiv.org/abs/2204.04901>.
- [17] Tosio Kato. *Perturbation Theory for Linear Operators*. Springer Berlin, Heidelberg, 1995. DOI: <https://doi.org/10.1007/978-3-642-66282-9>.
- [18] B. O. Koopman and J. V. Neumann. “Dynamical Systems of Continuous Spectra”. In: *Proceedings of the National Academy of Sciences of the United States of America* 18.3 (1932), pp. 255–263. ISSN: 00278424, 10916490. URL: <http://www.jstor.org/stable/86259> (visited on 11/13/2024).
- [19] Christian Kühn. “Lecture Notes on Dynamical Systems”. 2023.
- [20] Andrzej Lasota and Michael Mackey. *Chaos, Fractals, and Noise*. Springer New York, NY, 1993. DOI: <https://doi.org/10.1007/978-1-4612-4286-4>.
- [21] Vladimir Mironov et al. “A systematic study of minima in alanine dipeptide”. In: *Journal of Computational Chemistry* 40.2 (2019), pp. 297–309. DOI: <https://doi.org/10.1002/jcc.25589>.
- [22] Klaus-Robert Müller et al. “An introduction to kernel-based learning algorithms”. In: *Handbook of neural network signal processing*. CRC Press, 2018, pp. 4–1.
- [23] Feliks Nüske et al. “Markov state models from short non-equilibrium simulations—Analysis and correction of estimation bias”. In: *The Journal of Chemical Physics* 146.9 (2017). ISSN: 1089-7690. DOI: [10.1063/1.4976518](https://doi.org/10.1063/1.4976518). URL: <http://dx.doi.org/10.1063/1.4976518>.
- [24] Saburou Saitoh and Yoshihiro Sawano. *Theory of Reproducing Kernels and Applications*. Springer Singapore, 2016. DOI: <https://doi.org/10.1007/978-981-10-0530-5>.
- [25] D. Sarason. *The H^p Spaces of an Annulus*. American Mathematical Society memoirs. American Mathematical Society, 1965. ISBN: 9780821812563. URL: <https://books.google.de/books?id=ZLLTCQAAQBAJ>.
- [26] Cosma Shalizi. *Stochastic Processes, Lecture 25*. Online. 2006. URL: <http://www.stat.cmu.edu/~cshalizi/754/2006/>.
- [27] B. Simon. *Operator Theory*. American Mathematical Society, 2015. ISBN: 9781470411039.

- [28] Terrence Tao. *When are eigenvalues stable?* Online. 2008. URL: <https://terrytao.wordpress.com/2008/10/28/when-are-eigenvalues-stable/>.
- [29] Lloyd N. Trefethen and Mark Embree. *Spectra and Pseudospectra*. Princeton University Press, 2005. ISBN: 9780691213101. DOI: <https://doi.org/10.1515/9780691213101>.
- [30] Matthew O. Williams, Ioannis G. Kevrekidis, and Clarence W. Rowley. “A Data–Driven Approximation of the Koopman Operator: Extending Dynamic Mode Decomposition”. In: *Journal of Nonlinear Science* 25.6 (2015), pp. 1307–1346. ISSN: 1432-1467. URL: <http://dx.doi.org/10.1007/s00332-015-9258-5>.
- [31] Matthew O. Williams, Clarence W. Rowley, and Ioannis G. Kevrekidis. *A Kernel-Based Approach to Data-Driven Koopman Spectral Analysis*. 2015. arXiv: 1411.2260 [math.DS]. URL: <https://arxiv.org/abs/1411.2260>.